



**HAL**  
open science

# Continental depositional record of climate and tectonic evolution around the Eocene-Oligocene transition in southeast France: perspectives from the Vistrenque Basin (Camargue)

Nazim Semmani, François Fournier, Jean-Pierre Suc, Séverine Fauquette, Michel Séranne, Philippe Leonide, Lionel Marié, Jean Borgomano

## ► To cite this version:

Nazim Semmani, François Fournier, Jean-Pierre Suc, Séverine Fauquette, Michel Séranne, et al.. Continental depositional record of climate and tectonic evolution around the Eocene-Oligocene transition in southeast France: perspectives from the Vistrenque Basin (Camargue). *Bulletin de la Société Géologique de France*, 2024, 195, pp.8. 10.1051/bsgf/2024005 . hal-04694615

**HAL Id: hal-04694615**

**<https://ifp.hal.science/hal-04694615v1>**

Submitted on 11 Sep 2024

**HAL** is a multi-disciplinary open access archive for the deposit and dissemination of scientific research documents, whether they are published or not. The documents may come from teaching and research institutions in France or abroad, or from public or private research centers.

L'archive ouverte pluridisciplinaire **HAL**, est destinée au dépôt et à la diffusion de documents scientifiques de niveau recherche, publiés ou non, émanant des établissements d'enseignement et de recherche français ou étrangers, des laboratoires publics ou privés.



Distributed under a Creative Commons Attribution 4.0 International License

# Continental depositional record of climate and tectonic evolution around the Eocene-Oligocene transition in southeast France: perspectives from the Vistrenque Basin (Camargue)

Nazim Semmani<sup>1,2</sup> , François Fournier<sup>1</sup>, Jean-Pierre Suc<sup>3</sup> , Séverine Fauquette<sup>4</sup> , Michel Séranne<sup>5</sup>, Philippe Léonide<sup>1</sup>, Lionel Marié<sup>1,\*</sup> and Jean Borgomano<sup>1</sup>

<sup>1</sup> Aix Marseille Université, CNRS, IRD, Cerege, Um 34, 3 Place Victor Hugo (Case 67), 13331, Marseille Cedex 03, France

<sup>2</sup> IFP Energies Nouvelles, 1-4 Avenue de Bois-Préau, 92852 Rueil-Malmaison, France

<sup>3</sup> Sorbonne Université, CNRS-INSU, Institut des Sciences de la Terre Paris, IStEP, UMR 7193, 75005 Paris, France

<sup>4</sup> Institut des Sciences de l'Évolution de Montpellier (ISEM), CNRS, Univ. Montpellier, IRD, EPHE, Montpellier, France

<sup>5</sup> Géosciences Montpellier, Université de Montpellier – CNRS, Montpellier, France

Received: 4 September 2023 / Accepted: 20 February 2024 / Publishing online: 23 May 2024

**Abstract** – Based on detailed sedimentological analyses of cores, interpretation of well logs and a set of geochemical measurements performed on lacustrine sedimentary rocks, the palaeoenvironmental evolution and the sedimentary architecture of the Paleogene continental Vistrenque Basin (SE France) have been reconstructed. The analysis of sedimentary archives revealed three main stages of basin infill evolution: (1) a deep-lake basin (Priabonian-earliest Rupelian) whose sedimentation was dominated by terrigenous gravity-driven deposits during a period of high subsidence rate and strike-slip fault activity and under a prevailing humid climate; (2) an evaporative deep lake (early Rupelian) characterized by a drastic reduction in lake volume (forced-regression), terrigenous supplies and deposition of evaporites in disconnected sub-basins; (3) an overall long-term normal regressive stage (middle Rupelian to earliest Chattian) of lake infill characterized by an increase in terrigenous supplies and a vertical upward transition from deep-lake gravity-driven deposits to marginal lake and floodplain sedimentation. The onset of lake volume reduction and forced regression during the early Rupelian is associated with (1) the reworking of marginal lake carbonates into the deep lake areas, (2) the deposition of organic-rich sediments (TOC > 10%) coupled with sulphate-reduction processes in the deepest areas of the lake, (3) an important decrease in terrigenous supplies and (4) a long-term increase in  $\delta^{18}\text{O}$  of matrix-supported carbonates. This early Rupelian forced regression of the Vistrenque lacustrine system is interpreted to result from a regional decrease in precipitation in response to global cooling during the Eocene-Oligocene Transition (EOT). The final infill of the Vistrenque lake system (late Rupelian-early Chattian) and the onset of a floodplain occurred in more humid conditions during a stage of decreased activity of the Nîmes Fault, prior to or during an early stage of the Liguro-Provençal rifting.

**Keywords:** Eocene-Oligocene transition / lake basin / strike-slip basin / Liguro-Provençal rifting / carbonates / gravity-driven sedimentation

**Résumé** – Archives sédimentaires continentales de l'évolution tectonique et climatique du sud-est de la France autour de la transition Eocène-Oligocène : le Bassin de la Vistrenque (Camargue). Une reconstitution de l'évolution paléoenvironnementale et de l'architecture sédimentaire du bassin paléogène de la Vistrenque (Sud-Est de la France) a été réalisée à partir de l'analyse détaillée de carottes de forage, de l'interprétation de diagraphies et de mesures géochimiques (isotopes stables du carbone et de l'oxygène, teneurs en matière organique et en carbonate). L'analyse des archives sédimentaires a révélé 3 étapes principales d'évolution du bassin : (1) une phase précoce à sédimentation lacustre profonde (Priabonien-Rupélien basal) à dominante gravitaire, pendant une période de fort taux-de subsidence et de climat humide ; (2) une phase ultérieure de réduction de volume du lac (régression forcée) au Rupélien inférieur, caractérisée par une baisse drastique des apports terrigènes et le dépôt d'évaporites dans des sous-bassins

\*e-mail: [fournier@cerege.fr](mailto:fournier@cerege.fr)

compartimentalisés et déconnectés ; (3) une phase de régression normale du lac et de comblement du bassin (Rupélien moyen à Chattien inférieur), exprimée par une transition verticale de dépôts lacustres profonds gravitaires à des dépôts marginaux puis de plaine d'inondation. L'initiation de la réduction de volume du lac au Rupélien inférieur et la phase de régression forcée est enregistrée par (1) l'érosion des bordures carbonatées du lac et leur remaniement dans les dépôts gravitaires profonds, (2) le dépôt de sédiments riches en matière organique (COT > 10%) couplé à des processus de sulfato-réduction bactérienne, (3) une diminution significative des apports terrigènes et (4) une tendance à l'augmentation du  $\delta^{18}\text{O}$  des carbonates lacustres. Cet épisode de régression forcée est la conséquence d'un climat plus sec en réponse au refroidissement global de la transition Eocène-Oligocène. Le remplissage final du bassin lacustre et l'installation d'une plaine d'inondation s'est produit en contexte plus humide et de faible activité de la faille de Nîmes, au cours d'un stade précoce de la phase de rifting Liguro-Provençal ou antérieurement à celle-ci.

**Mots clés :** Transition Eocène-Oligocène / bassin lacustre / bassins sur décrochement / rifting Liguro-Provençal / carbonates / sédimentation gravitaire

## 1 Introduction

Continental sediments revealed to be very sensitive to climate changes because they result from physical or biological processes occurring in nearby areas or in direct contact with atmosphere (*e.g.*, Fabre and Mainguet, 1991; Nutz *et al.*, 2019). Among continental depositional systems, lakes have been shown to constitute comprehensive and reliable archives of the evolution of environmental parameters at various time scales due to fluctuations in their level which respond to climate and hydrologic changes and to the ability of biologically or chemically-produced carbonates to record palaeo-temperatures, pCO<sub>2</sub>, salinity and hydrologic balances (*e.g.*, Talbot, 1990; Tanner, 2010; Lettéron *et al.*, 2017). Additionally, sedimentation in continental basins is also extremely sensitive to tectonic setting like in shallow-marine setting (*e.g.*, Ashley and Renaut, 2002) since the latter controls the formation and location of reliefs and terrigenous sediment sources as well as those of subsident areas where sediments are deposited and preserved.

The time interval ranging from the Priabonian (Late Eocene) to the Rupelian (Early Oligocene) is marked at a global scale by the most important climate change of the Cenozoic resulting in the establishment of Antarctic ice sheets (Liu *et al.*, 2009) and records the transition from greenhouse to icehouse conditions (Wade *et al.*, 2012). In terrestrial mid-to-high latitude environments, long-term cooling during the Eocene-Oligocene transition (EOT) resulted in major changes in floristic and faunistic associations, and in regional hydrological cycles (Hutchinson *et al.*, 2021) but also promoted climate aridity (Yancey *et al.*, 2003; Page *et al.*, 2019) and seasonality (Eldrett *et al.*, 2009). Moreover, this period is characterized in Western Europe by a major transition in tectonic regime from compressional (Pyrenean compression) to extensional (European Cenozoic Rift System: ECRIS and Liguria-Provence extension) (Séranne *et al.*, 2021) which occurred coevally with the development of the marine Western Alps foreland basin to the east (Joseph and Lomas, 2004).

Late Eocene and Oligocene continental rift basins have been extensively documented in the literature concerning Western Europe, onshore (*e.g.*, Upper Rhine Graben: Blanc-Valleron and Schuler, 1997; Bresse Graben: Curial and Moretto, 1997; Valence Basin: Dromart and Dumas, 1997; Apt-Manosque-Forcalquier Basin: Lesueur, 1991; Alès-Saint-Chaptes-Issirac

basins (ASCI system): Lettéron *et al.*, 2017, 2018, 2022; Camargue Basin: Benedicto *et al.*, 1996) and offshore in the Gulf of Lion (Central Graben, Grand Faraman Basin: Séranne *et al.*, 1995) (see location in Fig. 1). These basins are characterized by thick siliciclastic, carbonate and evaporite sedimentation (*e.g.*, Benedicto, 1996; Rouchy, 1997).

The Vistrenque Basin is located in the western part of the Camargue area. It is the deepest Cenozoic continental basin in Southeast France with more than 3200 m thick Paleogene succession. This basin is bounded to the west by the Nîmes Fault (Figs. 1 and 2) which acted as a sinistral strike-slip fault as early as the Priabonian in Languedoc (Séranne *et al.*, 2021). This major fault may also have triggered the formation of the Vistrenque Basin during the Priabonian and Early Oligocene, a few million years before the Gulf of Lion extension. The Paleogene sedimentary infill of the Vistrenque Basin has been subdivided into three main units: the lowermost terrigenous-rich lacustrine 'Série Grise' Unit is more than 2000 m thick; an intermediate siliciclastic-rich fluvial 'Série Rouge' Unit, around 200 m thick; and an evaporite-rich 'Série Calcaréo-salifère' Unit, of few hundreds of metres thick, at the top (Fig. 3). Since the Série Calcaréo-Salifère Unit has been shown to be linked to the Upper Oligocene to Aquitanian rifting (Benedicto *et al.*, 1996; Semmani *et al.*, 2023), this study focuses only on the ante-saliferous units, namely the Série Rouge and underlying units.

The density of subsurface data (cores, cuttings, well logs) from the Gallician and Pierrefeu sectors (see location in Figs. 2A and 3B) makes it possible to investigate the sedimentary record and the tectonic evolution of the Vistrenque Basin during the transition from the Pyrenean compressional stage to the rifting of the Gulf of Lion margin, and to document the record of the well-known global climate change at the Eocene-Oligocene transition in continental environments from Southwestern Europe. The present study aims to: 1) define the depositional facies and reconstruct the depositional palaeoenvironments, 2) reconstruct the evolution of depositional systems and patterns of the Paleogene sedimentary infill of the Vistrenque Basin, 3) link the evolution of these depositional systems to changes in climate and tectonic regimes in Southeast France during the Priabonian-Rupelian times, and 4) discuss the relevance of continental sedimentary records as archives of past climate changes in Southwestern Europe around the Eocene-Oligocene transition.

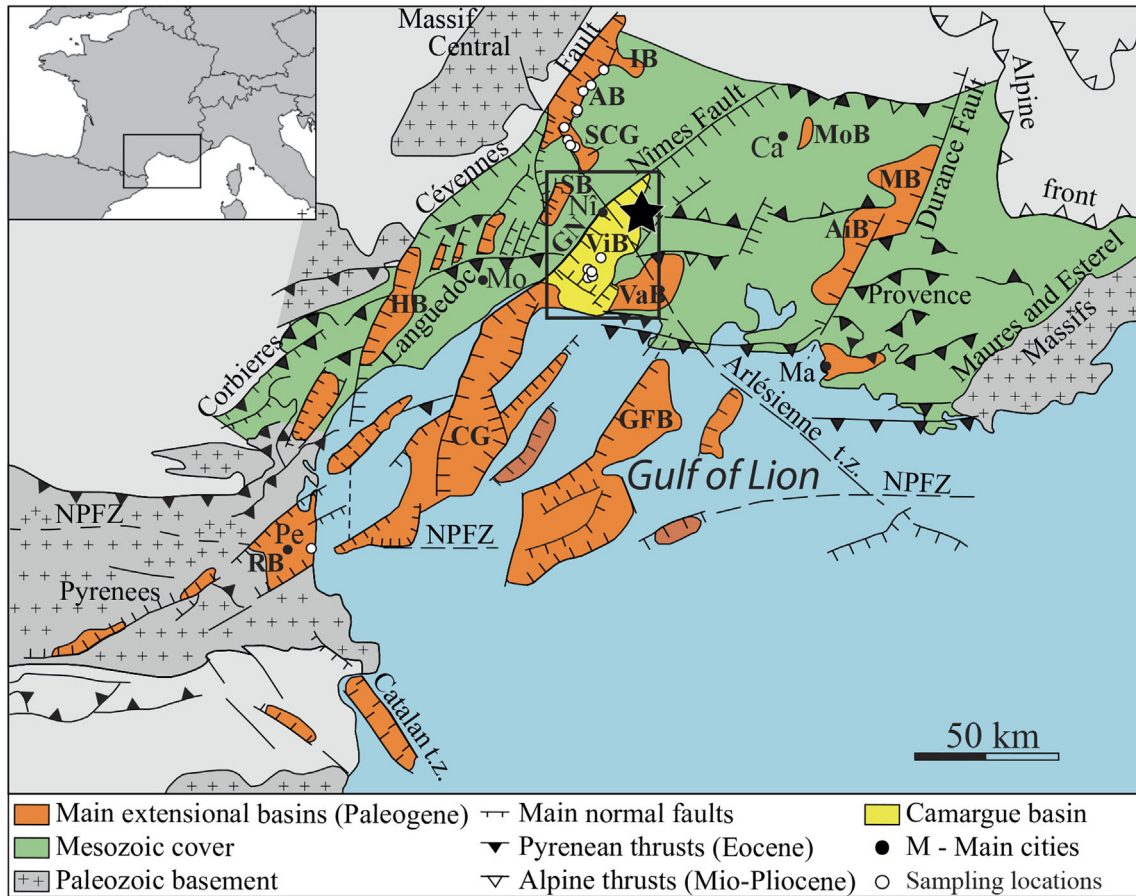


**Fig. 1.** Structural map of Southeast France and location of the Vistrenque Basin among the many Cenozoic continental basins, modified after [Benedicto \(1996\)](#). AB: Alès Basin, AiB: Aix Basin, Ca: Carpentras, CG: Central Graben, GFB: Grand Faraman Basin, GN: Garrigues Nîmoises, HB: Hérault Basin, IB: Issirac Basin, Ma: Marseille, Mo: Montpellier, MB: Manosque Basin, MoB: Mormoiron Basin, Nî: Nîmes, NPFZ: North Pyrenean Fault Zone, Pe: Perpignan, RB: Roussillon Basin, SB: Sommières Basin, SCG: Saint-Chaptes Graben, t.z.: transfer fault zone, VaB: Vaccarès Basin, ViB: Vistrenque Basin. The black star indicates the position of the Priabonian northern carbonate succession at Butte Iouton (*e.g.*, [Pellat and Allard, 1895](#); [Semmani \*et al.\*, 2022](#)).

## 2 Geological setting

### 2.1 Regional tectonic setting

The Camargue area is located in Southeast France, near the Rhône Delta, between the limestone plateaus of the ‘Garrigues Nîmoises’ and the Mediterranean ([Fig. 1](#)). This area has an approximately triangular shape and is constituted of two Cenozoic sedimentary basins that are entirely buried beneath the Rhône Delta sediments: the Vistrenque Basin to the west and the Vaccarès Basin to the east ([Fig. 1](#)). As a result of the convergence and collision of the Iberia-Corsica-Sardinia block with the European plate, the Mesozoic to Eocene cover has been folded and thrustured during the Pyrenean shortening in Languedoc and Provence (*e.g.*, [Mascle \*et al.\*, 1994](#); [Arthaud and Laurent, 1995](#); [Séranne \*et al.\*, 1995](#); [Bestani \*et al.\*, 2015](#)). The Paleogene Vistrenque Basin (50 \* 30 km<sup>2</sup>) is controlled by the major Nîmes Fault and is one of the many continental basins that opened during the late Eocene and the Oligocene in Southeast of France ([Cavalier \*et al.\*, 1984](#), [Semmani \*et al.\*, 2023](#)). These basins resulted from the Priabonian-Rupelian

Western European Rift extension (ECRIS, [Ziegler, 1992](#)) and the Oligocene-Aquitainian Liguria-Provence rifting ([Benedicto \*et al.\*, 1996](#)) in Languedoc, Provence, Rhône Valley and Gulf of Lion areas ([Fig. 1](#)). In Languedoc, the Nîmes Fault has been shown to accommodate sinistral strike-slip movements as early as the Priabonian in response to both the Pyrenean shortening and Western European Rift extension ([Séranne \*et al.\*, 2021](#)).

The Mesozoic substratum is constituted mainly of Jurassic and Cretaceous marine carbonates and is exposed in the ‘Garrigues Nîmoises’ ([Fig. 1](#)). These carbonates also constitute the buried structural highs that bound the Paleogene Vistrenque Basin to the east (Albaron high; Jurassic), to the north (Jonquières high; Lower Cretaceous), and to the south (Grau-du-Roi and Saintes-Maries highs; Jurassic) ([Fig. 2](#)). The Palaeozoic basement is known from the Massif Central, and Provençal Maure and Esterel massifs. Offshore in the present Gulf of Lion, the Paleozoic basement was intersected by Paleogene extensional basins (*e.g.*, Grand Faraman Basin, Central Graben) formed during the Oligocene-Aquitainian extension ([Séranne \*et al.\*, 1995](#)). Recently, [Séranne \*et al.\* \(2021\)](#) have reconstructed a Pyrenean relief, south of Camargue and

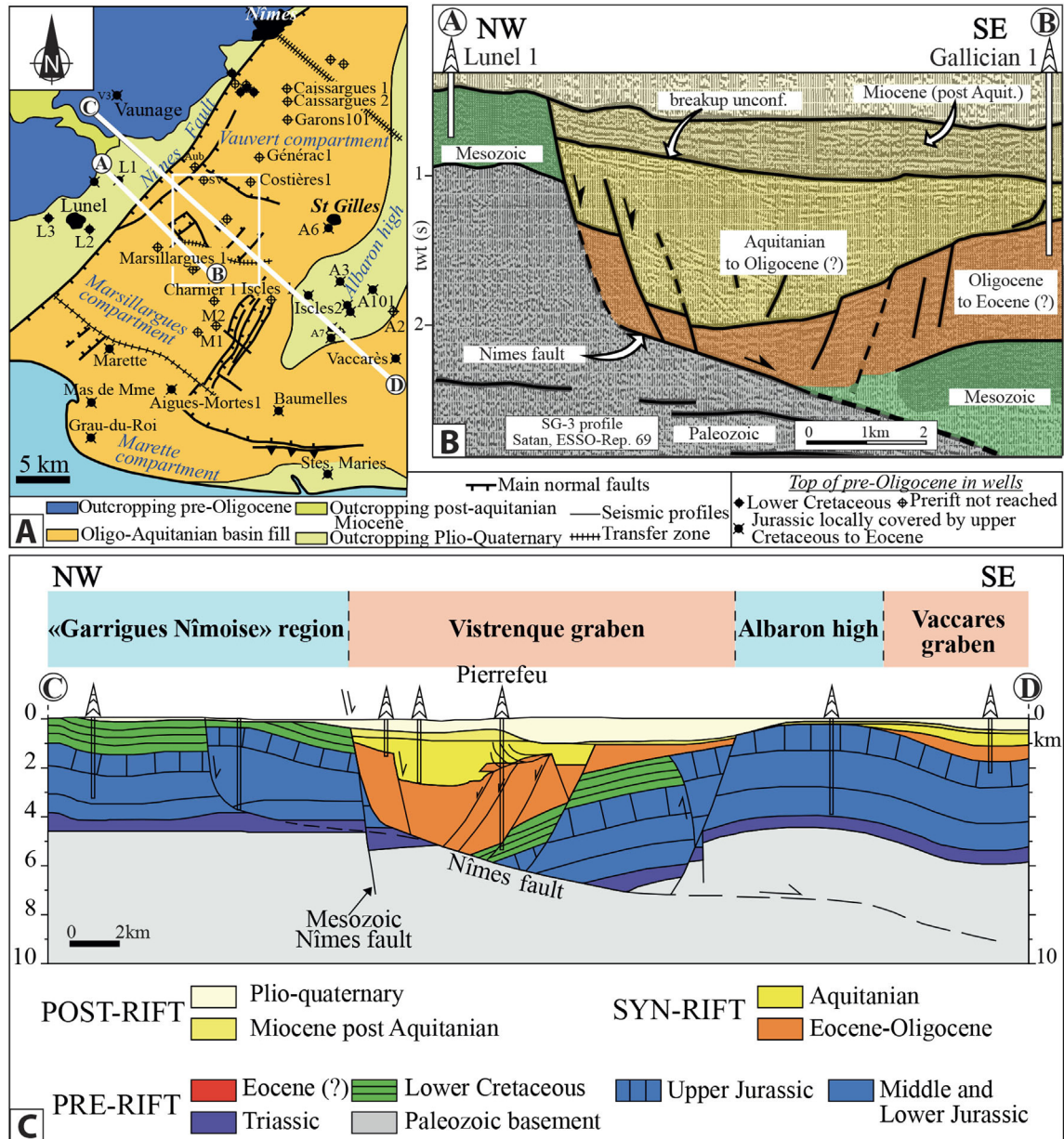


**Fig. 2.** (A) Structural map of the Vistrenque Basin showing the location of the deep boreholes, modified after [Benedicto \*et al.\* \(1996\)](#). A101: Albaron 101 – A2: Albaron 2 – A3: Albaron 3 – A6: Albaron 6 – A7: Albaron 7 – A-Mortes 1 : Aigues-Mortes 1 – Aub: Aubord 1 – Char 1: Charnier 1 – Csg 1,2: Caissargues 1,2 – L1: Lunel 1 – L2: Lunel 2 – L3: Lunel 3 – LJ: La Jasette – M1: Montcalm 1 – M2: Montcalm 2 – P: Pierrefeu 1 – P: Pierrefeu 1 – Stes Maries: Saintes-Maries-de-la-Mer 101 – SV: Saint-Véran 1 – V3: Vaunage 3. t.z.: transfer zone. The rectangle shows the studied area (Pierrefeu and Gallician sectors, north and south to the transfer zone respectively) shown in the geographical map of [Figure 3B](#). (B) Non-migrated seismic profile SG3 interpreted, after [Benedicto \(1996\)](#), location in (A) is indicated by the AB transect; (C) NW-SE cross-section through the Vistrenque Basin on the northern Vauvert compartment (modified after [Benedicto \*et al.\*, 1996](#), see location in A): CD transect).

Languedoc that links the French-Spanish Pyrenees to the Provence segment of the Pyrenean orogen and dated the onset of its dismantling to the Priabonian (late Eocene).

## 2.2 Stratigraphic framework of the Vistrenque Basin

Except for the Priabonian carbonate succession exposed at the Butte Iouton hill (black star on [Fig. 1](#)) in its Northern

margin ([Pellat and Allard, 1895](#); [Semmani \*et al.\*, 2022](#)), the Paleogene sedimentary succession of the Vistrenque Basin is almost entirely buried beneath the Miocene deposits and the Pliocene and Quaternary sediments of the Rhône Delta. Within the Vistrenque Basin, the Paleogene stratigraphic column changes laterally in both lithologies and thicknesses between the different sectors, particularly between the Gallician and Pierrefeu sectors, since the basin is affected by transfer faults

resulting in its compartmentalization (Fig. 2A). In the Pierrefeu sector, the Paleogene succession (~3200 m thick) has been subdivided into three main lithological units, from bottom to top: ‘Série Grise’, ‘Série Rouge’, and ‘Série Calcaréo-salifère’ formations (Valette and Benedicto, 1995) (Fig. 3A).

Very recently, Semmani *et al.* (2023) provided a revised chronological framework for the Paleogene of the Vistrenque Basin. In the Gallician sector (Fig. 3A), the lowermost lacustrine-dominated ‘Série Grise’ and ‘Série Calcaire’ formations are Priabonian to Middle Rupelian in age. The overlying fluvio-lacustrine ‘Série Mixte’ and ‘Série Rouge’ formations are late Rupelian to early Chattian in age. The return to lacustrine conditions resulted in the deposition of a thick carbonate and evaporite succession (‘Série Calcaréo-Salifère’ Formation) (*e.g.*, Valette and Benedicto, 1995) which is attributed to the Upper Oligocene to Aquitanian time interval by Semmani *et al.* (2023).

Seismic data interpreted by Valette (1991) suggest that the Série Calcaréo-Salifère Formation unconformably overlies the Série rouge and underlying units. Chronostratigraphic data (Semmani *et al.*, 2023) revealed that such unconformity can be dated to the early Chattian. Syn- Gulf of Lion rifting sedimentation lasted until the late Aquitanian and the break-up event that separates syn-rift from post-rift deposits was dated to the Burdigalian and corresponds to the spreading of the Liguro-Provençal Basin (Gorini *et al.*, 1993). The post-Aquitanian Miocene and Pliocene-Quaternary correspond to the post-rift stage of the Gulf of Lion margin (Figs. 2B and 2C; Séranne *et al.*, 1995).

## 3 Database and methods

### 3.1 Database

Borehole data were acquired by oil companies (SNPLM, CEP: former companies currently incorporated into Total-Energies) as part of the petroleum exploration in the Gallician sector in the 1950’s and later during a development drilling survey with the Pierrefeu 1 well drilled in 1963. Since the 1970’s, salt mining using halite leaching led to the drilling of more than 20 well doublets in the Pierrefeu sector in order to extract brine from the thick evaporite accumulation of the Série Calcaréo-Salifère Formation (Fig. 3B). However, these wells are not considered in this work since the studied intervals (Série Rouge Formation and underlying units) have not been reached.

This study is based on data from 6 wells (cores and drilling cuttings, well logs, geological reports) from the Gallician and Pierrefeu sectors: Gallician 1, Gallician 3, Gallician 7, Gallician 9, Vauvert 1, and Pierrefeu 1 (see location in Fig. 3B). All these wells have reached the Série Rouge Formation and intersected partially to totally the underlying units. The maximum depth, the deepest explored stratigraphic levels, and the available well log data and geological reports are summarized in Table 1.

Many wells were not considered in this study (*e.g.*, Gallician 2, 4, 5, 6, and 8) due to lack of core data. However, the studied wells, listed in Table 1 are a representative selection of the sedimentary record of the Paleogene of the Vistrenque Basin. Figure 4 provides a correlation panel of the Paleogene sections from these wells.

### 3.2 Depositional facies and palaeoenvironmental interpretations

The definition of the depositional facies is based on the description of the sedimentological features observed both macroscopically on cores and microscopically on thin sections (>1000 thin sections were examined). The thin sections were made by the geological departments of the oil companies during the 1950’s and 1960’s. The thin sections dataset was prepared with a close vertical spacing (ranging from 5 cm to 1 m).

Microscopic analyses on thin sections were carried out essentially semi-quantitatively in order to define the depositional facies (Tab. 2). Semi-quantitative analysis includes estimation of average grain size, grain sorting and morphological features, and proportion of fines (carbonate mud and silt). The definition of the depositional facies is also based on the identification of biological content, sedimentary structures, stratal patterns, and vertical stacking patterns. Depositional palaeoenvironments are interpreted from the depositional facies grouped within facies associations (FA, Tab. 3) and from their vertical evolution.

The carbonates have been described using the Dunham classification system (Dunham, 1962) modified by Embry and Klovan (1971) and the terrigenous deposits have been classified using the granulometric classification of Wentworth (1922).

### 3.3 Stable carbon and oxygen isotope analyses of carbonates

Carbon and oxygen stable isotopes compositions of bulk-rock carbonates have been measured on 117 samples from Gallician 9 well, 89 samples from Pierrefeu 1 well and 35 samples from Vauvert 1 well in order to provide insights into lake palaeohydrology. Measurements have been performed on matrix-supported fabrics (calcareous claystones, marlstones, argillaceous limestones and limestones of mudstone-wackestone textures) from the ‘Série Grise’, ‘Série Calcaire’ and ‘Série Mixte’ formations. Carbon and oxygen stable isotopes signatures of carbonates from the ‘Série Mixte’ and ‘Série Rouge’ units are altered by the intense pedogenic modifications that these limestones underwent and are therefore not considered. The isotope analyses were performed at the Laboratory of Analytic Geochemistry of the Faculty of Earth Sciences at Friedrich-Alexander-University of Erlangen-Nürnberg, Germany. Carbonate powders were reacted with 100% phosphoric acid at 70 °C using a Gasbench II connected to a ThermoFisher DELTA V Plus mass spectrometer. All values are reported in per mil relative to V-PDB. Reproducibility for  $\delta^{13}\text{C}$  and  $\delta^{18}\text{O}$  was  $\pm 0.07\text{‰}$  and  $\pm 0.05\text{‰}$  (1 standard deviation), respectively. Carbon and oxygen stable isotope measurements have been reported in Supplementary data – Table S1.

### 3.4 Organic matter and CaCO<sub>3</sub> concentrations

The present work integrates unpublished measurements of total organic matter content (TOC) and calcimetric analyses from oil companies inhouse reports. The TOC measurements

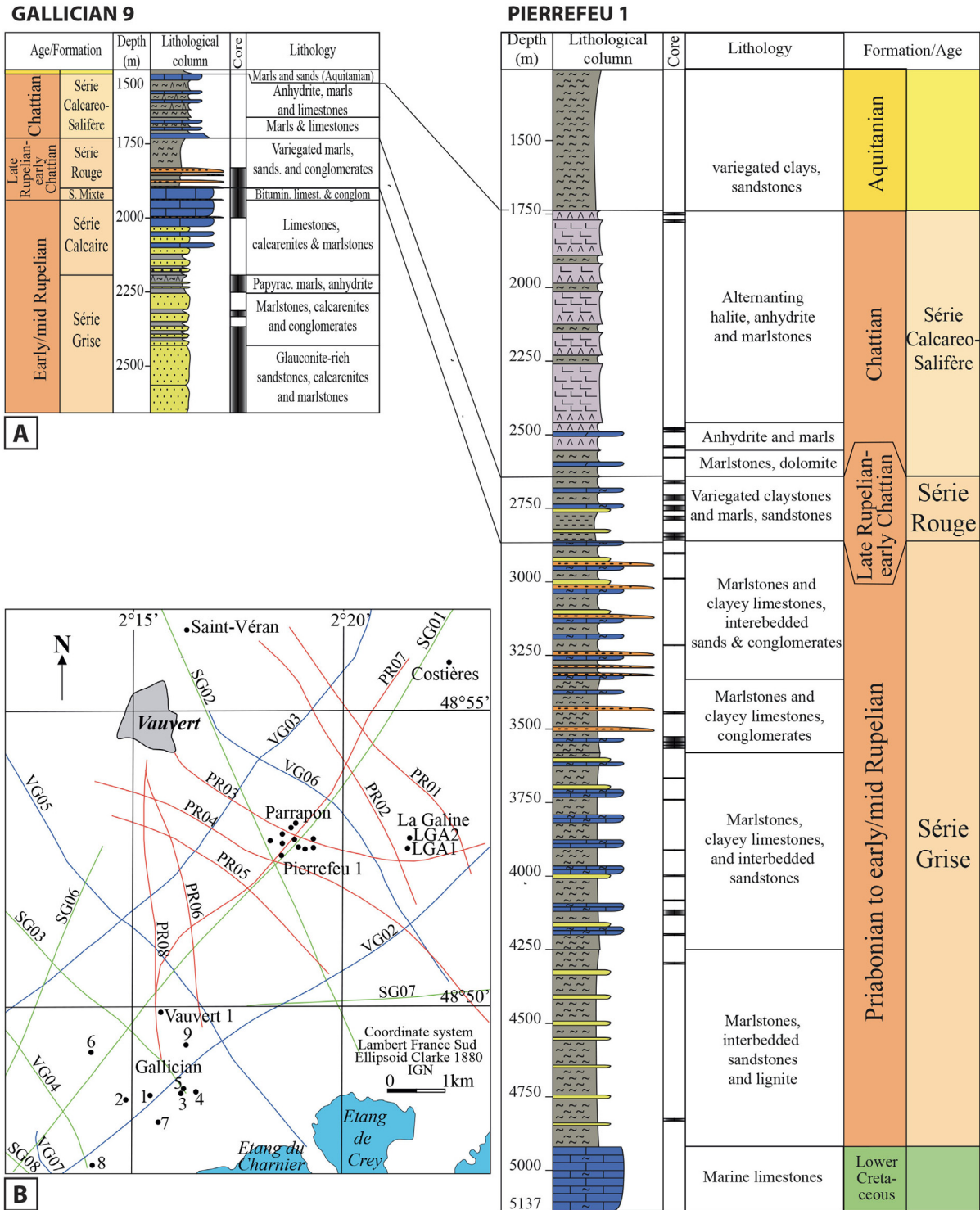


**Fig. 3.** (A) lithological columns and correlations of the Gallician 9 and Pierrefeu 1 wells located in the Gallician and Pierrefeu sectors respectively and chronostratigraphic framework after Semmani *et al.* (2023); (B) Geographical map of the Gallician and Pierrefeu sectors (enlargement of the rectangle shown in Fig. 2A) showing the location of subsurface database (wells and seismic lines), LGA = LaGaline well; numbers refer to the Gallician wells (from Gallician 1 to Gallician 9), modified after Valette (1991).

**Table 1.** List of boreholes studied in this work and the dataset used. Core intervals are indicated for the Paleogene series, Fm: formation (see location in Fig. 3B).

Well	Location	Year of completion	Depth (reached formation)	Dataset (well logs, documents)	Cores and cuttings data
Gallician 1	Vauvert (Gard)	1951	2004 m (Série Rouge Fm)	Electrical logs, Gamma Ray (GR), geological reports, master-log	Cores: 1612 – 1929 m
Gallician 3	Vauvert (Gard)	1951	1871 m (Série Mixte Fm)	Electrical logs, Gamma Ray (GR), geological reports, master-log	Cores: 1720 – 1871 m
Gallician 7	Vauvert (Gard)	1952	2087 m (Série Mixte Fm)	Electrical logs, Gamma Ray (GR), geological reports, master-log	Cores: 2007 – 2087 m
Vauvert 1	Vauvert (Gard)	1952	3626 m (Série Grise Fm)	Electrical logs, Gamma Ray (GR), geological reports, master-log	Cores, essentially: 1897 – 2014 and 2902-3067 m
Gallician 9	Vauvert (Gard)	1956	2653 m (Série Grise Fm)	Electrical logs, Gamma Ray (GR), geological reports, master-log	Cores: 1830 – 1997 / 2190 – 2247 / 2365- 2653 Cuttings: 2000-2190 m
Pierrefeu 1	Vauvert (Gard)	1963	5137 m (Lower Cretaceous) Base of Paleogene: 4920m	Electrical logs, Gamma Ray (GR), geological reports, master-log	Discontinuous cores between 1740 and 4830 m

have been performed in 1992 at the IFP (French Institute of Petroleum) using a Rock Eval apparatus and following the methodology established by Espitalié *et al.* (1985). The data are displayed in Supplementary data – Table S2.

### 3.5 Sequence stratigraphy analysis and well correlations

Sequence stratigraphy analysis was carried out at the metric to decametric scale in the cored intervals. High-resolution depositional cycles are defined using vertical evolution of facies associations. Since the studied formations are very thick and fine-scale correlations between the wells are difficult to make, only the major sedimentary cycles recorded during the Paleogene in the Vistrenque Basin will be described.

Well correlations are based on lithological criteria and well log data (Gamma Ray), the recognition of transgressive-regressive cycles and the identification of the major unconformities from the vertical stacking pattern, and the vertical evolution of carbon and oxygen isotope composition of lacustrine carbonates and the corresponding long-term trends of inflow-evaporation balance. Sequence boundaries have been defined as major, correlatable subaerial exposure surfaces or may correspond to conformable surface of maximum regression of the lake (basinal relative conformity).

## 4 Results and interpretations

### 4.1 Depositional facies and palaeoenvironmental interpretations

In the studied wells, the investigated Paleogene intervals display a great diversity of depositional facies including strictly terrigenous, carbonate and evaporite-rich deposits as well as mixed terrigenous-carbonate deposits. Thirteen depositional facies (F1 to F13) have been described, their main characteristic features and palaeoenvironmental

interpretations are summarized in Table 2. Due to the difficulty to capture large-scale sedimentary geometries in drill cores, interpretations of detrital carbonates and siliciclastics in terms of depositional environments are based on the vertical and distribution of facies (F1 to F13) and on their facies associations (FA1 to FA6, Tab. 3).

#### 4.1.1 Hemipelagic lacustrine marls and evaporite facies: F1, F2 and F3

##### F1. Anhydritic marlstones and anhydrite

Anhydritic marlstones and banded anhydrite are uncommon facies within the studied intervals since these are reported only from the upper part of the “Série grise” Formation. Anhydritic marlstones consist of dark-grey marls encasing sparse nodules of anhydrite (up to 2 cm in size, Fig. 5) while banded anhydrite consists of centimetre-thick layers of nodular anhydrite, alternating with thin, millimetre-thick, micrite laminae (Fig. 5B). Anhydrite has also been observed infilling fractures. The anhydritic marlstones are organized in two plurimetre thick intervals of finely laminated platelet marls intercalated with fine silty sandstones and organic-rich layers. The banded anhydrite interval (~ 1 m thick) is bracketed between those two anhydritic marlstones intervals. In thin section, anhydrite nodules display a microcrystalline structure made of little needle crystals (Fig. 5C). A few relicts of small prismatic to lenticular crystals have been evidenced within anhydrite nodules (Fig. 5D) thus suggesting a gypsum precursor.

**Interpretation:** The nodular habit of the anhydrite is a common diagenetic fabric thus does not necessarily indicate subaerial sabkha environments (Dean *et al.*, 1975). The occurrence of relicts of pseudomorphs after gypsum crystals suggests that laminated anhydrite derives from the diagenetic transformations (under burial conditions?) of laminated gypsum deposits. The original alternation of gypsum and organic-rich carbonate layers reflects fluctuations between more and less arid



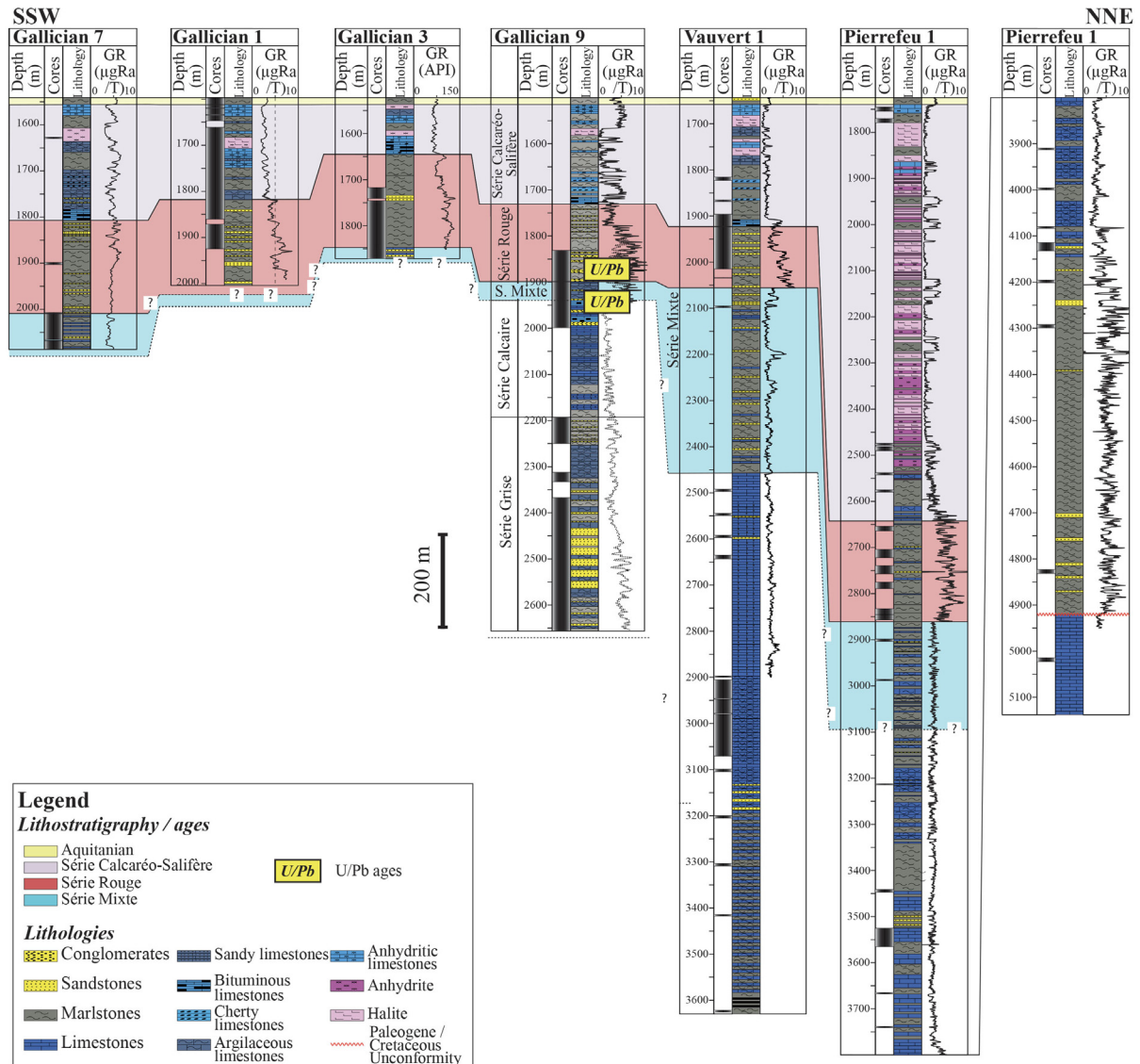


**Fig. 4.** Correlation panel of wells Gallician 7, Gallician 1, Gallician 3, Gallician 9, Vauvert 1 and Pierrefeuf 1 from the Gallician and Pierrefeuf sectors showing the sedimentary units, lithologies and lithostratigraphic correlations. Lithostratigraphic correlations are carried out using lithological similarities and gamma ray (GR) signal.  $\mu\text{gRa}/\text{T}$ : microgram of Radium/Time (radioactivity measurement).

conditions leading to precipitation of these minerals on a shallow perennial lake floor while the nodular texture results from subsequent diagenetic transformation of gypsum into anhydrite (Orti and Salvany, 2004). Large and scattered prismatic anhydrite crystals embedded in a marlstone background are likely to form and grow within the mud matrix during early diagenesis, prior to mud lithification. As discussed by Semmani *et al.* (2023), sulphate may derive from the leaching of triassic evaporites in the catchment area of the lake or from transient marine water incursions.

**F2. Finely laminated argillaceous limestones and papyraceous marlstones (laminites)**

This facies consists of alternations of light beige and dark grey, greenish grey and brown finely laminated argillaceous limestones and papyraceous marlstones. Laminae are often

millimetric to submillimetric in thickness, plane-parallel to wavy and may also be crumpled (Fig. 5E). The dark layers are enriched in organic matter and in detrital particles of mud to silt size. In contrast, light laminae are dominated by micrite, and display low detrital and organic matter content. Preserved fossils are lacking in this facies although the papyraceous marlstones may contain high amounts of terrestrial plant debris intercalated between the laminae. These laminites are organized into thick intervals with a thickness ranging from several decimetres to few metres. This facies is particularly frequent in the upper part of the “Série Calcaire” and less frequent in the upper part of the “Série Grise” Formation while the lowermost intervals of the “Série Grise” are devoid of it.

**Interpretation:** The fine grain-size in the laminates indicates deposition in areas located far from the clastic sources. The lack of fauna suggests anoxic conditions, and the preservation of the original laminae indicates that they have

**Table 2.** Depositional facies classification of the Paleogene sedimentary succession of the “Série rouge” and underlying formations in the Vistrenque Basin: biological contents, sedimentary and diagenetic features, and their palaeoenvironmental interpretations.

Code	Facies	Biological content	Sedimentary structures	Stratal pattern	Diagenetic features	Occurrence	Palaeoenvironmental interpretation
F1	Anhydritic marlstones and anhydrite	--	Nodular and banded structure	Metre anhydrite banded interval enclosed between anhydrite marlstones	Replacement of gypsum by anhydrite	Uncommon, reported only from one thick interval from “Série grise” Formation	Evaporitic perennial lake
F2	Finely laminated limestones and papyraceous marlstones	Terrestrial plant remains	Millimetre laminations Wavy to plane-parallel	Several decimetres to metre thick intervals	--	Frequent in the “Série calcaire” & occasional in the “Série grise”	Profundal perennial lake with anoxic condition
F3	Dark grey marlstones with scarce fauna	Terrestrial plant remains, few ostracod shells	Structureless	Massive and structureless interval. Frequent alternations with the F4 sandstones	Occasional pyrite precipitation	Common in the “Série Grise” and in the Série calcaire Formations	Profundal perennial lake with poorly oxygenated conditions
F4	Glauconite-rich sandstones and fine calcarenites	Azoic. Terrestrial plant remains	Plane parallel laminations and current ripples. Load casts and flame structures	Centimetre to few cm layers in alternation with marlstones/siltstones	--	Common in the “Série grise” Formation	Gravity-driven currents in the offshore lake
F5	Coarse calcarenites and microconglomerates	Azoic. Terrestrial plant remains	Vertical normal grading, parallel laminations	Centimetre to decimetre beds overlying F3 marlstones and overlain by F4 sandstones	--	Frequent in the upper part of the “Série grise” Formation	Gravity-driven currents in the offshore lake
F6	Matrix-supported conglomerates	Mostly azoic. Occasional characean grains in the matrix	--	Decimetre beds intercalated with F3, F4 and F5 facies	--	Occasional to frequent in the “Série grise” Formation	Gravity-driven currents in the offshore lake
F7	Thinly-bedded quartzose calcarenites	Azoic. Few terrestrial plant remains	--	Decimetre tabular beds to metre beds. May alternate with F2 marlstones and display subaerial exposure features	Pedogenic modifications at the top of the beds including desiccation cracks	Frequent in the upper part of the “Série calcaire” but also at the base of the “Série mixte” Formation	Vicinity of a riverine mouth (lacustrine delta) with local detrital fluxes
F8	Oncolitic limestones	--	--	Decimetre to metre beds with subaerially exposed tops	Pedogenic modifications at the top of the beds including desiccation cracks	Occasional in the “Série mixte” Formation	Shallow lake littoral and riverine mouth in the lake
F9	Microbial limestones	microbial crusts (?)	--	Metre thick beds in alternation with palustrine carbonates (F13)	Occasional incipient pedogenic modifications (cracking)	Frequent in the “Série mixte” & “Série calcaire” Formations	Littoral lake in the vicinity of streams and springs
F10	Polymictic Conglomerates and microconglomerates	Azoic	Erosive base (?), grading into F11 and F12 facies. Preferential clast imbrication	Inframetric to metre beds alternating with sandstones and marlstones (F11/F12)	Occasional pendular cements and micrite coating around clasts	Frequent in the “Série rouge” and less frequent the “Série mixte” Formation	Bed load fill of channels

**Table 2.** (continued).

Code	Facies	Biological content	Sedimentary structures	Stratal pattern	Diagenetic features	Occurrence	Palaeoenvironmental interpretation
F11	Fine to medium sandstones (Quartzose sandstones)	Azoic.	Vertical normal grading, Current ripples (?)	Decimetre to metre beds in alternation with F10 and F11 facies	--	Common in the "Série rouge" and occasional in the "Série mixte" Formations	Slowdown of fluvial stream deposits, overbank deposits
F12	Variegated and mottled calcareous claystones	Azoic	--	Metre to several metres intervals alternating with F10, F11 and F13 facies	Mainly pedogenesis: root traces, marmorisation vermicular mottling & vivid red coloration, peds	Common in the "Série rouge" and "Série mixte" Formations Occasional in the "Série calcaire" Formation	Floodplain deposits
F13	Brecciated limestones (pedogenically modified carbonates)	Undetermined molluscs, ostracods	--	Decimetre to few decimetres beds. Often, pedogenesis modify the top of F7/F8/F9 and F12 facies beds	Pedogenesis: perigranular cracks, root traces, pseudo-microkarst, vadose pisoids may also be found. Geopetal silt and blocky calcite in cavities	Frequent in the "Série rouge" and occasional in the "Série mixte" (lowermost parts) and "Série calcaire" Formation	Very shallow pond/lake or abandoned channel subjected to exposure and vegetation development

**Table 3.** Depositional facies associations of the Paleogene ‘Série rouge’ and underlying units (‘Série mixte’, ‘Série calcaire’, ‘Série grise’) from the Vistrenque Basin (Camargue, SE France) defined in the Gallician and Pierrefeu sectors and their palaeoenvironmental interpretations.

Facies association	Facies Code	Depositional facies	Occurrence	Palaeoenvironmental interpretation
<b>FA1 Evaporite-rich perennial lake</b>	F1	Anhydritic marlstones and anhydrite	Uncommon, reported only from one thick interval from “Série grise” Formation.	<b>Evaporative perennial lake</b>
<b>FA2 Profundal lake</b>	F2	Finely laminated argillaceous limestones and papyraceous marlstones	Frequent in the “Série calcaire” Formation & occasional in the “Série grise” Formation	<b>Profundal perennial lake with poorly oxygenated conditions</b>
	F3	Dark grey marlstones with scarce fauna	Common in the “Série grise” and in the “Série calcaire” formations	
<b>FA3 Lake slope and offshore lake</b>	F4	Glauconite-rich sandstones and fine-grained calcarenites	Common in the “Série grise” Formation	<b>Gravity-driven currents in the lake slope and offshore lake</b>
	F5	Coarse calcarenites and microconglomerates	Frequent in the upper part of the “Série grise” Formation	
	F6	Matrix-supported conglomerates	Occasional to frequent in the “Série grise” Formation	
<b>FA4 Deltaic and littoral lake</b>	F7	Thinly-bedded quartzose calcarenites	Frequent in the upper part of the “Série calcaire” Formation but also at the base of the “Série mixte” Formation	<b>Vicinity of a riverine mouth (lacustrine delta) and lake littoral</b>
	F8	Oncolitic limestones	Occasional in the “Série mixte” Formation	
	F9	Microbial limestones	Frequent in the “Série mixte” and “Série calcaire” Formations	
<b>FA5 Fluvial association</b>	F10	Polymictic conglomerates and microconglomerates	Frequent in the “Série rouge” and less the “Série mixte” Formation	<b>Channelized and overbank deposits</b>
	F11	Fine to medium sandstones (Quartzose sandstones)	Common in the “Série rouge” and occasional in the “Série mixte” Formation.	
<b>FA6 Floodplain association</b>	F12	Variegated and mottled calcareous claystones	Common in the “Série Rouge” and “Série mixte” formations and occasional in the “Série calcaire” Formation.	<b>Floodplain and very shallow pond/ephemeral water pans</b>
	F13	Nodular-brecciated limestones (Pedogenically modified carbonates)	Frequent in the “Série mixte” and occasional in “Série rouge” (lowermost parts) and “Série calcaire” Formation.	

not been affected by bioturbation. The preservation of organic matter also suggests stratified water preventing oxygenation of the lake bottom. Finally, the absence of subaerial exposure features (*e.g.*, root traces) in these marlstones indicates deposition in deep and perennial lake conditions.

### F3. Dark grey marlstones with scarce fauna

Marlstones are very common in the “Série Grise” Formation and are found occasionally in the “Série Calcaire” and “Série Mixte” formations. F3 facies occurs in massive and structureless intervals in alternation with calcarenites and conglomerates (F4 to F7 facies, see description hereinafter) (Fig. 5F). These marls may contain significant amounts of silt-sized quartz and mica particles (=silty marlstones), and minor proportions of coarse detrital grains. Laminations are lacking and the marls are organic-rich thus resulting into the grey to dark grey colour; terrestrial plant remains are sometimes frequent. Preserved carbonate biotic remains are very scarce and consist mainly of ostracod shells (Fig. 5G). Pyrite is also reported from these marlstones.

**Interpretation:** The detrital fraction is made of fine-sized particles (silt, clay) indicating sedimentation in quiet areas located far from the sources hence in distal and central parts of a perennial lake. Preservation of organic matter as well as the extreme scarcity of carbonate skeletal grains suggests low oxygen conditions on the lake bottom as observed in ancient and modern perennial lakes with water stratification (Basilici, 1997). The occurrence of pyrite is also consistent with anoxic conditions in a lake bottom affected by sulphate reduction processes (Peckmann *et al.*, 1999). These dark grey marlstones are therefore interpreted to form in the distal, deeper, and poorly oxygenated areas of a lake which is subjected to detrital fluxes carrying the fine grains and the plant remains.

#### 4.1.2 Gravity-driven lacustrine facies: F4, F5 and F6

##### F4. Glauconite-rich sandstones and fine-grained calcarenites

F4 facies occurs within the “Série Grise” Formation and consists of moderately to well-sorted, fine mixture dominated by angular quartz, oxides minerals, glauconite and mica grains with reworked miscellaneous siliceous and carbonate elements. The latter include small-sized peloids and broken bioclasts (*e.g.*, benthic foraminifera, bryozoans, and echinoderms) derived from the reworking of Mesozoic marine limestones cropping out in the catchment area, as well as *microcodium* debris likely reworked from the neighbouring Paleogene continental limestones (Figs. 6A, D–G). Terrestrial plant remains are common whereas coeval lacustrine carbonate grains are scarce and could be represented by only a few ooids or peloids and characean remains. Sedimentary structures are represented by plane parallel laminations and current ripples (Fig. 6). At the core scale, these sandstones may also grade downwards into medium-sized sandstones and upwards into siltstones and marlstones (F3 facies, Fig. 6A–C). These sandstones may occur in several centimetres thick intervals (Fig. 6B) but also frequently alternating with marlstones in the form of millimetre to few centimetres thick layers thus forming banded intervals (Fig. 6C; “banded sandstones” *sensu* Lowe and Guy, 2000). In such banded

sandstones, the bounding surfaces of the layers may be erosive with rip-up clasts (Fig. 6B) and may exhibit soft sediment deformation and load structures such as flame structures and pendulous load cast (Fig. 6B and C).

##### F5. Coarse calcarenites and microconglomerates

Coarse-grained quartzose calcarenites and microconglomerates are reported mostly from the upper part of the “Série Grise” Formation. Clasts are made of various lithologies including limestones, sandstones, and more rarely siliceous elements (Fig. 7A). Rip-up elements are also found among these grains (Fig. 7A). In F5 facies, carbonate grains are essentially lithoclasts or fragments of marine bioclasts (*e.g.*, foraminifera, echinoderms, bryozoans) which can be found within the lithoclasts or as separate grains within the sandy matrix thus suggesting that they are reworked. The microconglomerates generally display a grain-size break with the subjacent marlstones (F3 facies) and may show parallel laminations and grade upward into medium and fine sandstones. This facies occurs generally in several centimetres to few decimetres thick intervals intercalated between the sandstones (F4 facies) and the silty marlstones (F3 facies).

##### F6. Matrix-supported conglomerates

This facies consists of sub-rounded to angular poorly sorted clasts, ranging in size from several millimetres to 1 cm and that reach up to 3 cm for the coarsest elements, embedded within a marlstone or silty sandstone matrix (Fig. 7B). F6 intervals show neither grading nor internal bedding. In the lower and middle parts of the “Série Grise” Formation, conglomerates are oligomictic and clasts generally consist in light grey marly limestones of Mesozoic age bearing a clearly defined Mesozoic fauna associated with some quartz grains and reworked calcite spars (Fig. 7C). In the upper part of this unit, the conglomerates are also oligomictic and the matrix may contain lacustrine carbonate grains (Fig. 7D). The conglomerates and breccias are found in alternation with the F2, F3 and F4 facies described in the previous sections.

##### Interpretation of F4, F5 and F6 facies

In the “Série Grise” Formation, F4 sandstones are characterized by good sorting and grading, and they display sedimentary structures such as parallel laminations and current ripples (Fig. 6A). These sedimentary structures are described together in the turbidite sequence of Bouma (1962): the parallel laminations are reported from the sandy level Tb, and the current ripples are indicative of the Tc interval. Such sedimentary structures and vertical stacking of facies have been associated with turbidity currents (Bouma, 1962, Tinterri *et al.*, 2020).

The presence of preserved plant fossils and the interbedding of the F4 sandstones with the F3 marlstones together with the lack of subaerial features suggest deposition in perennial lake conditions. The abundance of marine carbonate clasts, including bryozoans and reworked Mesozoic foraminifera (*e.g.*, *Cuneolina*), together with siliceous elements (sponge spicules) and glauconite mineral grains, suggests feeding from the erosion of the Mesozoic sedimentary cover that constitutes the neighbouring catchment area. Part of the siliciclastic

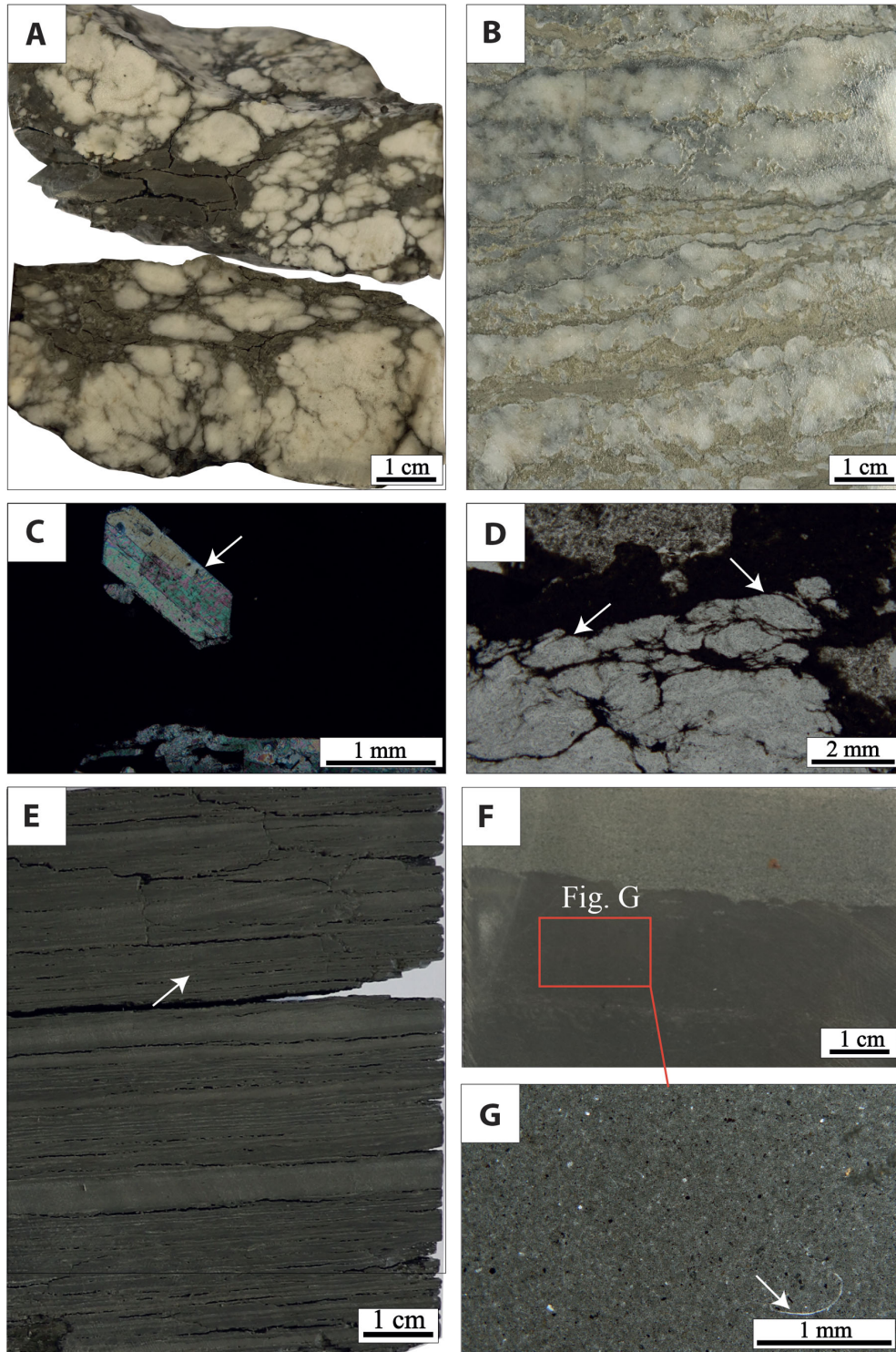


**Fig. 5.** Anhydritic marls and anhydrite (F1), finely laminated limestones and papyraceous marlstones (F2), dark grey marlstones with scarce fauna (F3) facies. (A) and (B) Hand sample images showing the whitish anhydrite nodules set in the marlstone matrix (A) and the banded anhydrite resulting from the coalescence of the anhydrite nodules (B). (C) Thin section of the facies F1 showing the needle microcrystalline structure of the anhydrite nodules (white arrow) embedded in a marlstone background (XPL image). (D) Thin section of the banded anhydrite (F1 facies) displaying the relicts of prismatic to lenticular crystals (white arrows) within the anhydrite nodules (PPL). (E) Core photograph showing the alternation of white and dark millimetre-thick laminae within the papyraceous marlstones (F2 facies), the white arrow indicates accumulation of horizontally settled plant leaves. (F) Hand sample showing a dark grey marlstone (Facies F3) interval that lies below a grey sandstone interval (further detailed images on sandstones in Fig. 6). (G) Microphotograph showing a close-up view of the box in (F) and displaying the microscopic characteristics of the dark grey marlstones (facies F3), the arrow indicates an ostracod shell.

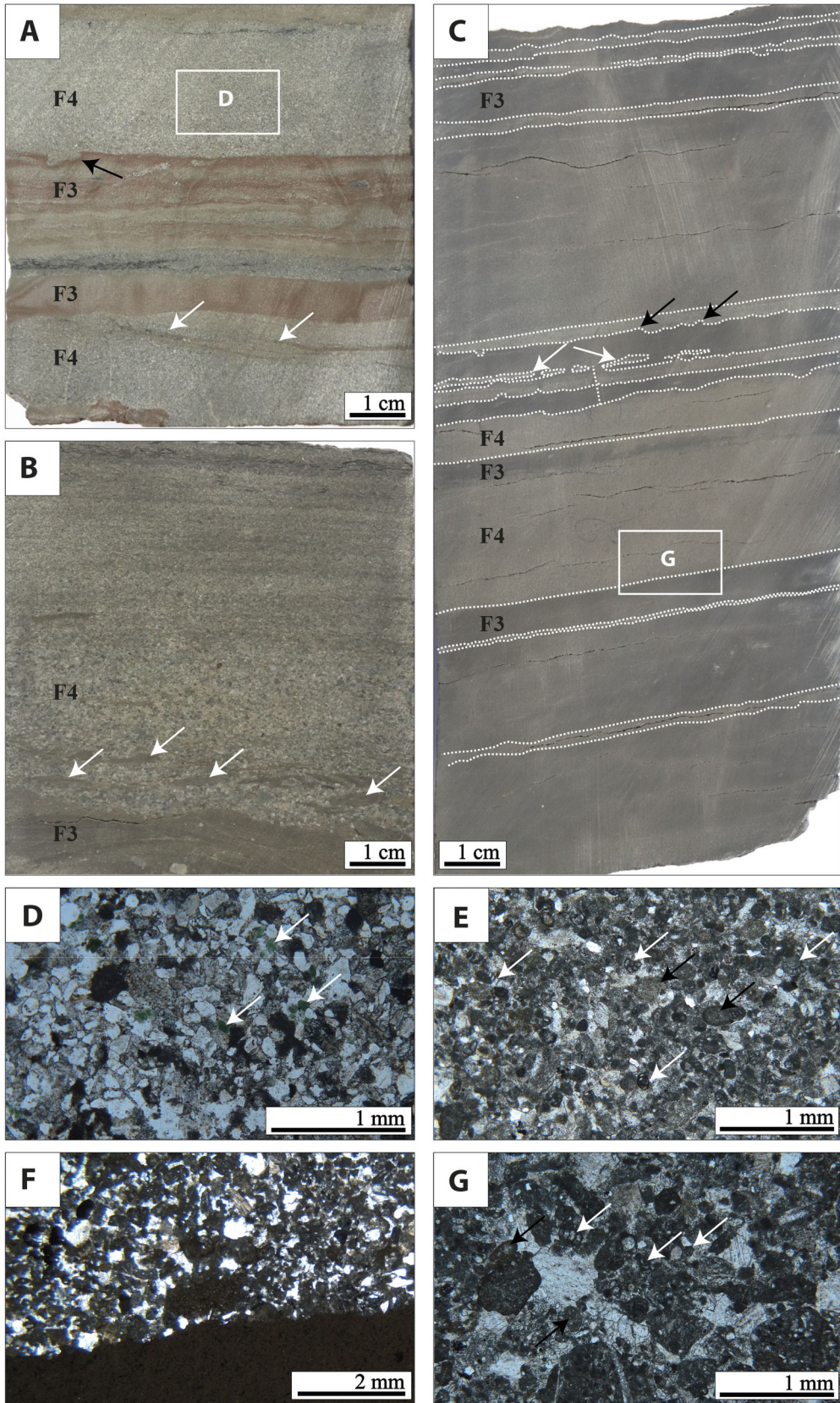


**Fig. 6.** Glauconite-rich sandstones and fine calcarenites (F4 facies). (A) Core photograph of glauconite-rich sandstone (F4 facies) alternating with marlstone/siltstone similar to those described previously (F3) in the form of planar parallel laminations similar to the upper parallel laminations of the Td member of the Bouma sequence (Bouma, 1962). The white arrows indicate current ripples within the sandstones similar to those from the Tc layer of the Bouma sequence, and the black arrows indicate a flute cast. As an indication, the direction of the current would be from the left to the right of the picture. Darker areas in the core sample indicate the accumulation of leaves. (B) Hand sample of fine to medium sandstone (F4 facies) displaying parallel lamination (lower parallel laminations of the Tb level of a Bouma sequence) with an erosive base and grain size cut-off with the underlying marlstone layer (F3 facies). The white arrows in F4 facies indicate rip-up clasts ripped from the F3 facies marls. (C) Core photograph displays alternation of the glauconite-rich sandstones (F4) and marls/siltstones (F3). Load structures are indicated by the arrows: white arrows indicate pendulous load cast while black arrows indicate flame structures. (D) Close-up view of the F4 sandstones from (A) showing the dominance of well sorted fine quartz and the abundance of glauconite mineral indicated by the white arrows (PPL microphotograph). (E) Thin section of the fine calcarenites (F4 facies) displaying the mixture of miscellaneous grains with the noticeable abundance of reworked Mesozoic foraminifera (white arrows) and the presence of lacustrine ooids/peloids (black arrows). (F) Thin section under PPL exhibiting a grain size cut-off between the calcarenite (F4 facies) and the underlying marlstone (F3 facies). (G) Thin section under PPL of a medium-sized calcarenite (F4 facies) displaying dominant carbonate extraclasts, some of which containing foraminifera (white arrows), the black arrow indicates a lacustrine ooid/peloid.

material supply, especially the quartz grains, may also be sourced from the dismantling of metamorphic and igneous rocks from distal areas (Pyrenean relief to the south and/or Cévennes Massif to the northwest).

The occurrence of F4 sandstones in alternation with dark grey marlstones (F3 facies) which together form the ‘banded sandstones’ intervals, displaying rip-up clasts, flame structures and pendulous load casts, suggest that F4 facies results from transitional gravity-driven flows in the deep parts of the lake (Haughton *et al.*, 2009, Tinterri *et al.*, 2020). Those soft sediment deformations have been described in marine-gravity driven sediments and have been interpreted to result from a transitional flow, the characteristics of which are intermediate between a cohesive flow and low-density current (Tinterri *et al.*, 2016, 2020).

The grain-size break with the underlying marlstones and the presence of parallel laminations within the coarse sandstones and microconglomerates (F5 facies) suggest a deposition resulting from density flow currents (Ta layer in Bouma (1962), S3 layer in Lowe (1982)).

In the F6 conglomerate facies, size and shape of carbonate clasts indicate low to moderate transport and the proximity of the source. Within these conglomerates, the occurrence of reworked lacustrine carbonate grains (*e.g.*, characean remains, ooids) suggests that the lake margins are also subjected to mechanical erosion during the deposition of these conglomerates. The poor sorting of the grains and the matrix-supported texture suggest *en masse* deposition as described by Tinterri *et al.* (2020). F6 facies is interpreted as resulting from the freezing of cohesive debris flows (Talling *et al.*, 2012, Tinterri *et al.*, 2020).

The F4, F5 and F6 facies are interbedded within the F3 marlstones and form hectometre-scale intervals in the Gallician sector which is located in the central part of the Vistrenque Basin. Haughton *et al.* (2009) related the different stratal morphologies and their sedimentary features (current and load structures, bedding geometry) to the basinward evolution of density current. F4, F5 and F6 are therefore interpreted to result from gravity-currents (hyperpycnal flow) that initiated on the slopes of the lacustrine basin and reached the deep areas of the lake. Similar stratal pattern within lacustrine gravity-driven deposits have been described in the

lacustrine delta front of the Ediacaran Camaquã Basin (Western Santa Bárbara Rift, Southernmost Brazil) and attributed to fluvial floods entering the lake system in the form of hyperpycnal flow (Lehn *et al.*, 2018).

#### 4.1.3 Terrigenous lake margin facies

##### F7. Thinly-bedded quartzose calcarenites

The bedded quartzose calcarenites occur mostly in the upper levels of the “Série Calcaire” formation and at the base of the “Série Mixte” Formation. In contrast to quartzose calcarenites from F5 facies which alternate with siltstones/marlstones in the form of centimetre layers, F7 facies forms massive decimetre to metre beds displaying pedogenic features on top (F13 facies) (Fig. 8E). In thin section, however, the F7 facies exhibits similar grain contents such as quartz and miscellaneous reworked grains from the Mesozoic carbonates.

**Interpretation:** The high content of carbonate clasts and quartz grains suggests high terrigenous flux in the depositional area. The carbonate grains are dominated by extraclasts sourced by the erosion of the Mesozoic cover from the neighbouring drainage area of the lake. The low matrix content (mud and silt) suggests winnowing of the sediment. However, the presence of pedogenic features (*e.g.*, cracking) at the top of the calcarenite beds indicate subaerial exposure. In addition, the occurrence of this facies in alternation with grey marlstones (F3 facies) and palustrine limestones (F13 facies, see description hereinafter) indicates the vicinity of the stream mouth and thus may be interpreted to be the delta or lacustrine shoreface deposits in the lake margin subjected to lake level fluctuations.

#### 4.1.4 Carbonate lake margin facies: F8 and F9

##### F8. Oncolitic limestones

Oncolitic limestones are found occasionally in the upper part of the “Série Calcaire” Formation. F8 facies is dominated by spherical to elongate oncoids and may be classified as a floatstone of oncoids according to the classification of Dunham (Dunham, 1962) modified by Embry and Klován (1971). In thin section, these oncoidal-rich carbonates display highly porous zones and the oncoids display fine micrite coatings



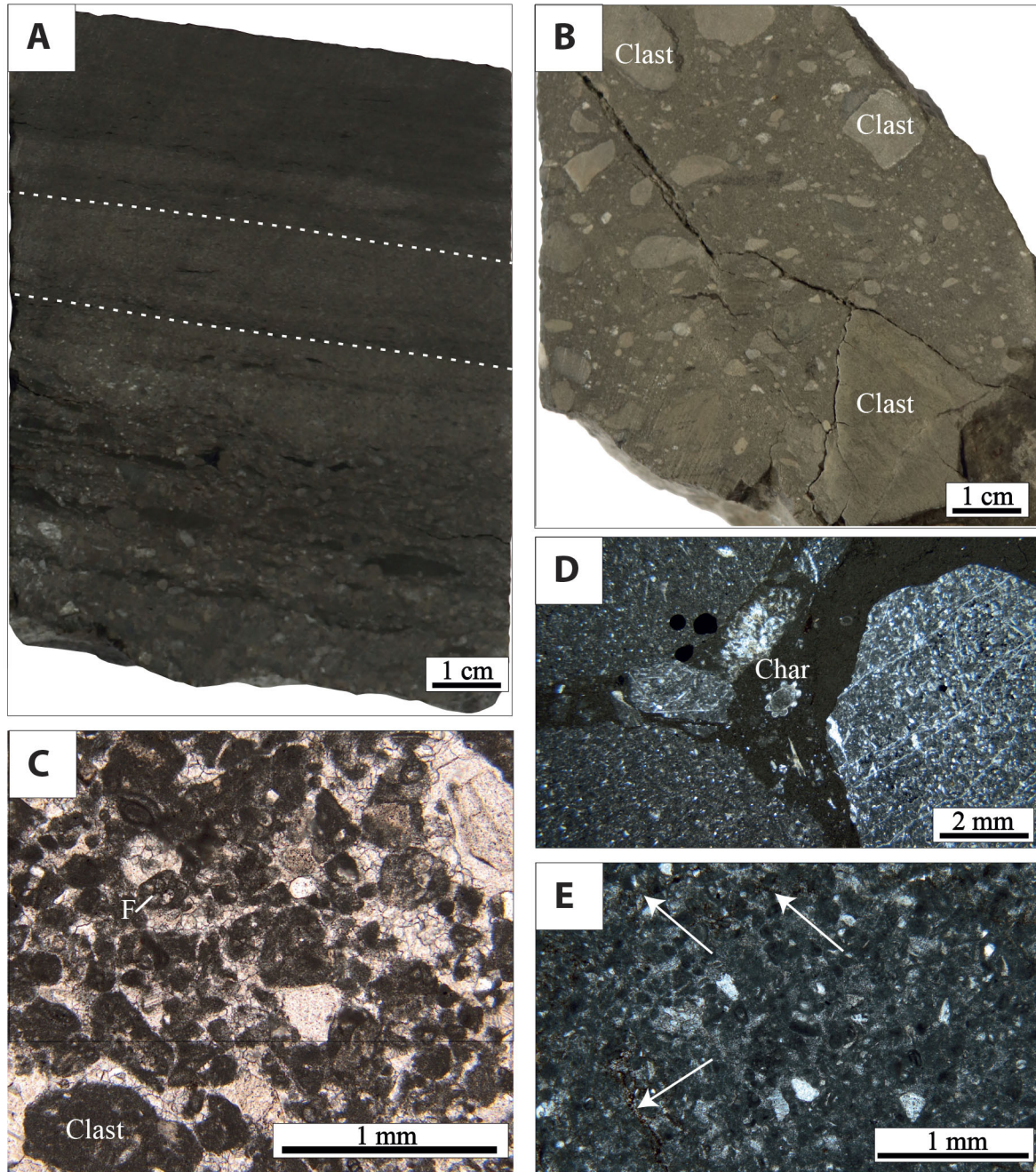


**Fig. 7.** (A) Core photograph showing the coarse calcarenite (F5 facies). Note that the base of the sample contains coarse grains while the grain size becomes finer at the top, the dashed lines indicate parallel lamination. (B) Core photograph showing a matrix-supported conglomerate with a particularly monomictic composition of the angular clasts (Clast). (C) Thin section of a sandy matrix showing the wide variety of reworked elements: foraminifera (F) and carbonate lithoclasts (Clast) (PPL). (D) Thin section under plane polarized light showing the nature of the clasts and the matrix. For instance, the clast on the right-hand side of the picture contains a marine limestone made of abundant sponge spicules. The marlstone matrix may contain lacustrine elements produced in situ like characean remains (Char). (E) Microphotograph under plane polarized light of a bedded quartzose calcarenite (F7 facies) from the upper interval of the “Série Calcaire” Formation. The detrital elements are similar to those from the previously defined calcarenites and microconglomerates. These calcarenites (F7 facies) are characterized by the presence of pedogenic features such as perigranular cracks (white arrows).

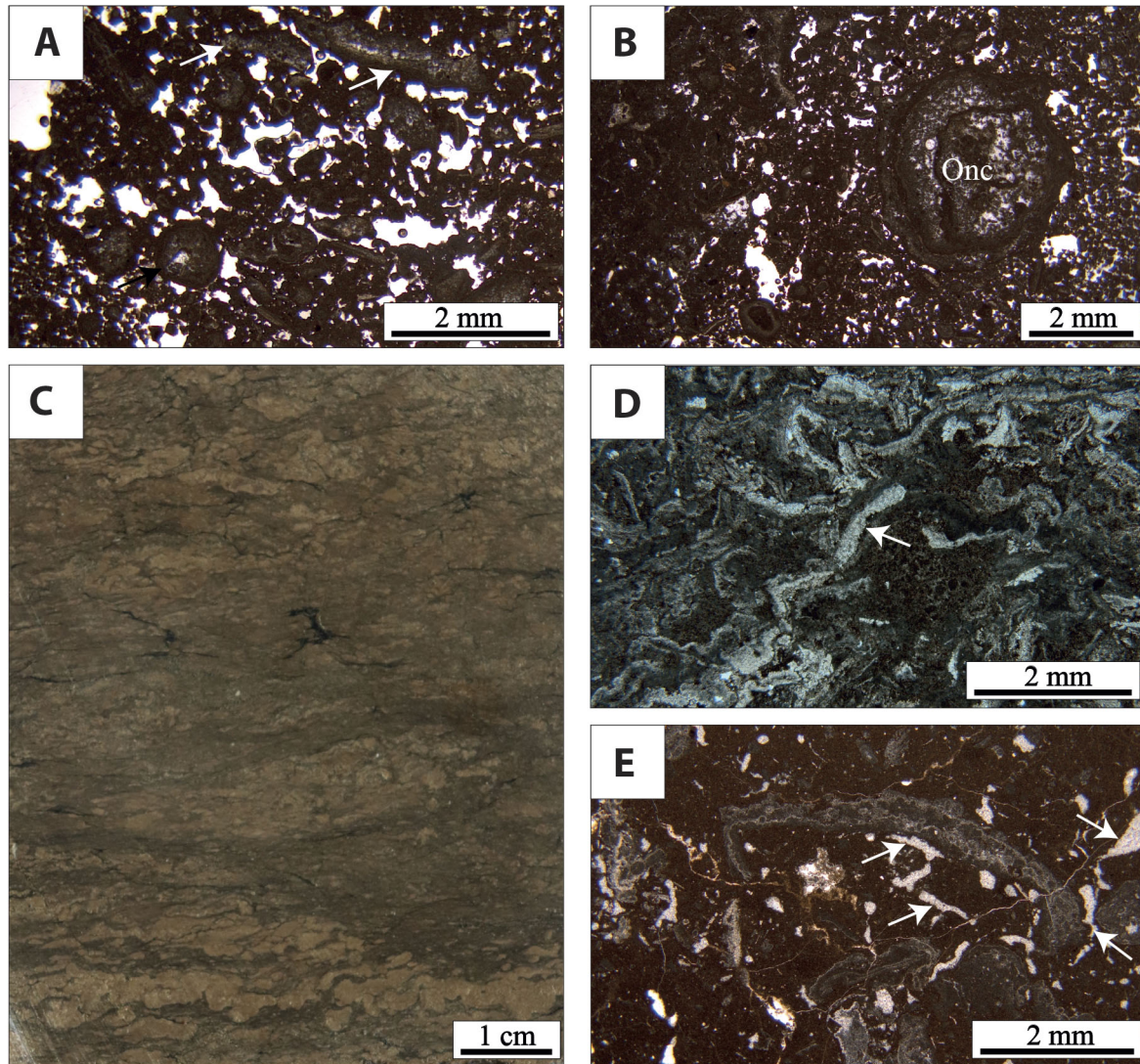


**Fig. 8.** Fluvial continental carbonate facies (F8 and F9). (A) Thin section of an oncolitic limestone (F8 facies) displaying various oncolid shapes, spherical (black arrow) and elongate (white arrows) within a interparticle porous zone. The texture of the limestone after the Dunham classification (Dunham, 1962) is floatstone to rudstone. (B) Detail of an oncolitic limestone showing the coatings of a spherical oncolite (Onc). (C) Core photograph showing beige microbial crusts (tufa fragments?) within a microbial limestone (F9 facies). (D) Microphotograph under plane polarized light showing microbial crusts (probably tufa fragments) that are non-organized and some of which look like broken crusts (white arrow). (E) Floatstone of microbial limestone (F9) showing micrite coating on thin grains (encrustations around leaves?). The white arrow indicates incipient pedogenic imprints expressed by the development of cracks filled with calcite.

(Fig. 8A-B). This facies occurs in the form of inframetric beds of brown vacuolar limestones, the top of which displaying pedogenic features such as circumgranular cracks and root traces. F8 limestones are found intercalated between red calcareous marlstones (F12 facies, see description hereinafter) and palustrine limestones (F13).

**Interpretation:** The occurrence of these limestones interbedded with red marlstones and palustrine limestones may suggest deposition in fluvial to nearshore lacustrine settings, possibly in the form of bed load infill of channel or overbank deposits in the fluvial system or as littoral deposits at the vicinity of a riverine mouth in a lake. Oncoids may

also have formed in spring or downstream fluvial environments and transported by flow toward a lake shore. The lack of matrix suggests strong hydrodynamic setting. The presence of pedogenic features on top of F8 beds indicates subaerial exposure and therefore confirms the shallow water setting which may be consistent with deposition in an ephemeral shallow lake setting. Oncolitic grainstones are reported from the margin of a saline lake setting in the neighbouring Priabonian Saint-Chaptes Basin (Lettéron *et al.*, 2018) while Arenas *et al.* (2007) described overbank oncolite-rich deposits in a floodplain from the Paleogene of Mallorca Island (Spain).

## F9. Microbial limestones

Microbial limestones occur in the form of metre-thick beds of brown vacuolar limestones made up of accumulation of millimetre to centimetre-scale microbial crusts with minor proportions of fine angular quartz (Figs. 8C and D). In thin section, these microbial limestones consist of irregularly arranged micrite and sparite millimetre laminae alternating with highly porous areas. The laminae are slightly broken (Fig. 8D) and show little displacement. Other features may include micrite encrustations around unpreserved elements (probably leaves). These limestones may display pedogenic modifications at the top of the beds including circumgranular cracking (Fig. 8E).

These limestones are frequent in the upper intervals of the “Série Calcaire” Formation and in the “Série Mixte” Formation. Microbial limestones are found in alternation with brecciated limestones (F13 facies defined hereinafter).

**Interpretation:** The presence of microbial crusts and encrustations (calcareous tufa) may indicate deposition in lacustrine, fluvial or water spring settings (Arenas *et al.*, 2010). Limestone bedrock availability is required to provide carbonate solutes to the fluvial system (Pentecost, 2005). The substratum of the Vistrenque Basin and the surroundings are dominated by Mesozoic marine carbonates thus making it possible for fluvial waters to be enriched in carbonate solutes. Tufa limestones can form within a broad range of climates (Arenas *et al.*, 2010) even though alternation of clear and dark laminae points to temperate to semi-arid climate (Viles *et al.*, 2007). However, tufa facies have been described from the fluvial and lacustrine settings from the Middle Eocene and Oligocene of Mallorca Island (Spain) (Arenas *et al.*, 2007 in Arenas *et al.*, 2010) under tropical and subtropical climate.

The limited displacement of microbial crusts indicates the vicinity of the location where these are formed to the lake littoral. The presence of mud matrix in these facies indicates rather a lacustrine depositional environment. Moreover, the presence of incipient pedogenic modifications suggests short-term subaerial exposure. The F9 facies is therefore interpreted to form within a lake littoral by reworking of carbonate crusts formed within nearby fluvial stream and spring waters emerging from a carbonate-rich bedrock.

### 4.1.5 Fluvial facies

#### F10. Polymictic conglomerates & microconglomerates

These conglomerates and microconglomerates are poorly sorted heterometric deposits and consist of a mixture of coarse sand to granule and pebble size gravels (Fig. 9A). The mean size of the clasts is 1 cm and the largest may reach up to 4 cm in size. The clasts are subangular to subrounded and are of diverse lithologies, these are dominantly made of quartz, feldspar, and mica, but also brown and beige limestone clasts of Mesozoic and Cenozoic ages with accessory glauconite (Fig. 9C). Some grains display anisopachous pendent cement and micrite coating (Fig. 9A). These polymictic conglomerates are clast-supported and have a sandy matrix made of fine to medium sandstones that infills the inter-clastic voids, the sandstones are medium-sized (average size ~ 1 mm). The conglomerates have no obvious internal grading or sedimentary features. Moreover, preferential imbrication is very crude or even roughly displayed.

F10 facies are frequent in the lower part of the “Série Rouge” Formation and are less frequent in the underlying “Série Mixte” Formation. Conglomerates are also present in the “Série Calcaire” but are mainly made of carbonate clasts and contains less terrigenous siliciclastic grains; these “monomictic” conglomerates have been described above (see F6 facies hereinbefore).

The terrigenous polymictic conglomerates are organized into inframetric to metric beds and are found in alternation with sandstones and marlstones (F11 and F12, see descriptions hereinafter). These conglomerates may grade upwards into medium and fine sandstones and then marlstones.

#### F11. Fine to medium sandstones (quartzose sandstones)

These sandstones are mainly made of very fine to medium-sized quartz grains with associated micas, feldspars, and glauconite/chlorite; less common centimetre-scale lithic mudstone fragments are also present (Fig. 9B). These quartzose sandstones are well to moderately sorted and carbonate mud fraction is very low or even lacking; dominant grain size ranges from 80 to 250  $\mu\text{m}$  (average ~ 170  $\mu\text{m}$ ) while the matrix may be constituted of silts and clays. Sandstones are azoic except the occurrence of scarce plant debris. In thin section, current ripples are highlighted by the orientation of sheet minerals (*e.g.*, mica, Fig. 9D).

F11 quartzose sandstones are common in the “Série Rouge” Formation and occur in decimetre to metre-thick beds in alternation with conglomerates and marlstones. This terrigenous facies becomes less frequent in the subjacent “Série Mixte” Formation and scarce or even absent in the lowermost “Série Calcaire” Formation. The sandstone beds of metric thickness may lie over conglomerate intervals and exhibit vertical normal (fining-up) grading to marlstones and thus form plurimetric stacks of conglomerates, sandstones and marlstones. However, in some cases, structureless fine sandstones may also occur as discrete and isolated decimetric beds interbedded with calcareous siltstones and claystones (F12 facies, see description hereinafter).

**Interpretation of F10 and F11 facies:** The clast-supported fabric of the conglomerates (F10 facies) suggests bed load transport within a channel. The wide range of the lithological nature of the clasts suggests feeding from both nearby and far sources. An example of nearby source includes tufa elements resulting from the erosion of contemporaneous upstream fluvial carbonates (Fig. 9D). The upwards grading of the conglomerates into sandstones (F11 facies) and calcareous claystones (F12 facies described hereinafter) reflects slow-down of fluvial currents, the energy of which gradually decreases allowing further deposition of fine sand grains and then fine particles (silts and clays), and therefore channel infill. F10 facies therefore represents deposition as bedload infill of braided and/or meandering streams in the proximal to central parts of the alluvial plain; the presence of outsize clasts would indicate more proximal (braided channels) areas of the alluvial plain.

The dominance of quartz, other silicates and metamorphic minerals in these polymictic conglomerates and siliciclastic sandstones indicates feeding from the weathering of crystalline rocks. Since the nearby catchment area of the basin is made

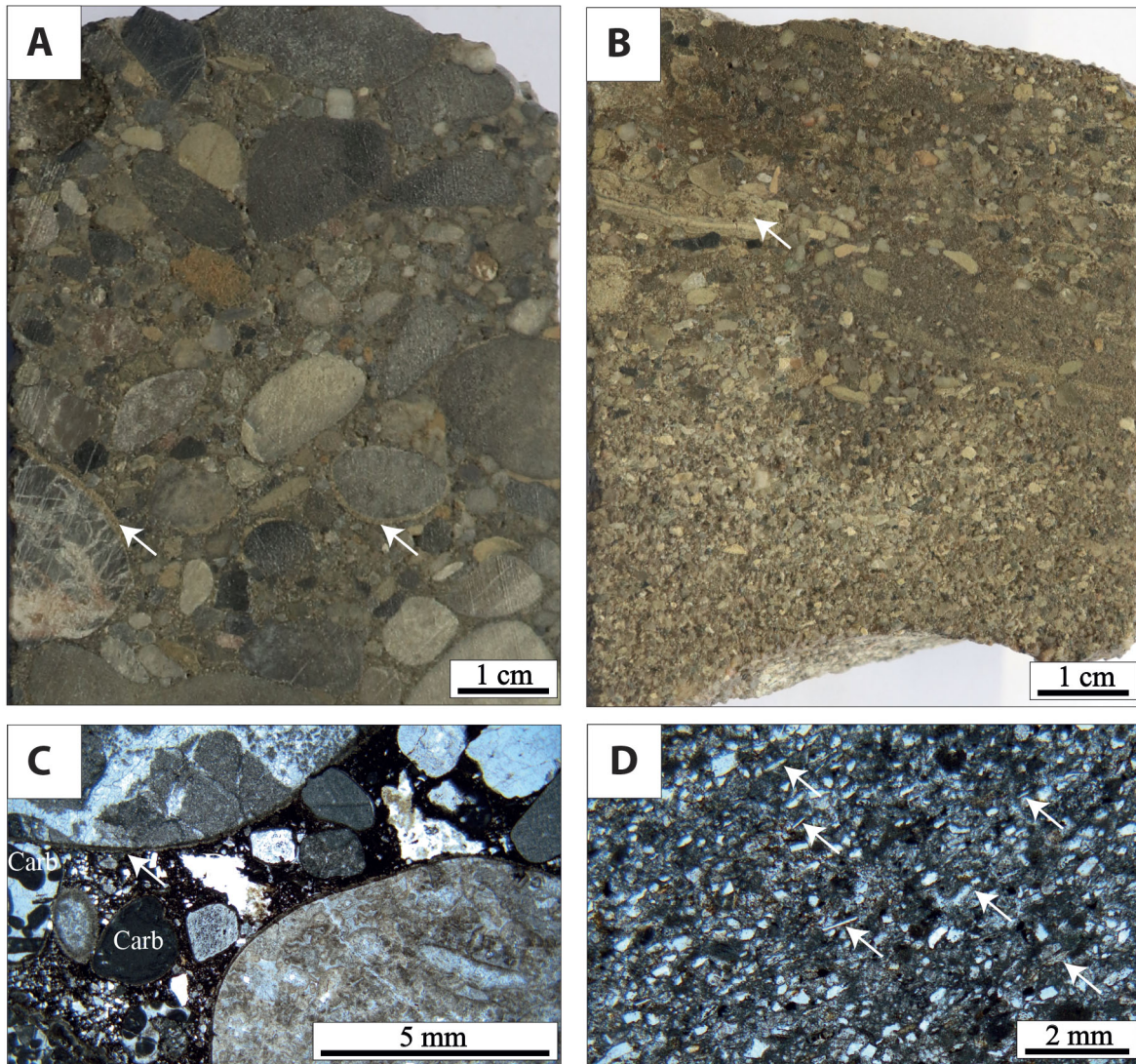


**Fig. 9.** Conglomerates (F10 facies) and sandstones (F11 facies). (A) Core photograph showing a polymictic clast supported conglomerate. The white arrows indicate pendant cements and/or micrite coating around the clasts. (B) Core photograph of a siliciclastic-rich sandstone (F11 facies). The lithic fragment indicated by the white arrow consists of a tufa clast (further details in Fig. 8). (C) Thin section showing the poor sorting of the clasts and the sandy matrix within the conglomerates F10 (Carb = carbonate lithoclasts). Notice the thin micritic coating around the grains. (D) Thin section photograph exhibiting the arrangement of sheet minerals (*e.g.*, mica) in F11 sandstones as outlined by the arrows and that may suggest current ripples (PPL).

essentially of Mesozoic carbonates and glauconite sandstones, the origin of the minerals, especially metamorphic, is to be found in the mountain ranges that were being dismantled at those times, probably the Pyrenees that bordered the basin to the South (Séranne *et al.*, 2021) or the Massif Central further to the northwest. Moreover, the relative abundance of polycrystalline quartz suggests a metamorphic origin for this mineral. The contribution of the Albian glauconite-rich sandstones to the feeding of the fluvial streams is very low or next to nil since glauconite mineral is rarely observed in the F10 and F11 facies in contrast to the glauconite-rich sandstone interval from the “Série Grise” where the high proportion of this mineral

suggests direct and significant feeding from the erosion from the regional Albian sandstones cover. Apart from the upwards grading into fine deposits, other evidence for fluvial deposition setting includes the presence of pedogenic features characteristic of alluvial plain in these claystones thus supporting the fluvial depositional setting for these conglomerates. In addition, sedimentary structures (current ripples) highlighted by the orientation of sheet minerals (*e.g.*, mica, Fig. 9D) in the sandstones suggest deposition by water stream. However, when the sandstones are found in the form of thin beds intercalated within the variegated claystones (F12 facies below), these rather represent overbank or sheet flood deposits in the floodplain.

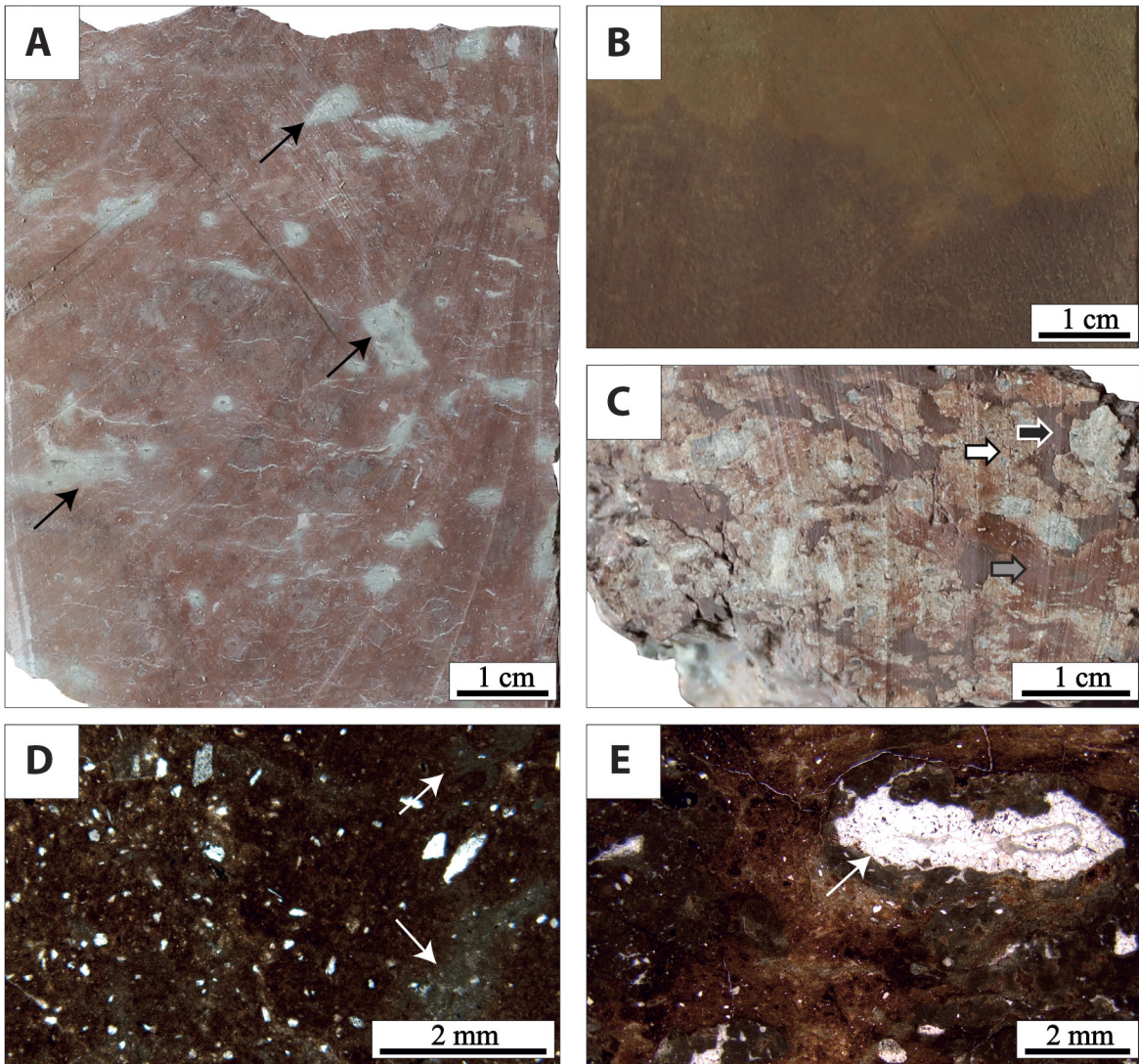


**Fig. 10.** Variegated and mottled calcareous claystones (F12 facies). (A) Core photograph from the “Série Rouge” formation showing a dominantly red calcareous claystone displaying green mottles (black arrows). (B) Core photograph showing different hues of red and orange colours within a sandy claystones (F12 facies). (C) Core photograph showing different ped structures with a broad palette of colours in the variegated marlstones with light pink (white arrow), dark red (grey arrow) and dark red-purplish (black arrow) clay matrix. (D) Thin section photograph showing green mottles (white arrows) within a dominantly brown sandy claystone (PPL). (E) Thin section photograph showing cross-cut root filled with blocky sparite (white arrow) within a variegated calcareous claystone (PPL).

#### 4.1.6 Floodplain and palustrine carbonate facies

##### **F12. Variegated and mottled calcareous claystones**

Lithofacies F12 consists of predominantly vivid red sandy calcareous claystones, variegated with brown, yellow, green, and occasionally orange colours (Figs. 10A–C). In thin section, these claystones are made up of very fine sand size (or silt size) siliciclastics including abundant quartz, feldspar, and mica (muscovite and biotite), with clays and oxides and very scarce glauconite. Silt is abundant (<30  $\mu\text{m}$  in size) while quartz grain size averages 50  $\mu\text{m}$  and coarser quartz grains (>100  $\mu\text{m}$ ) are found to be scattered within the silty matrix (Fig. 10D). F12 facies is in general azoic and displays marmorisation patches (mottling). Other pedogenic features

are found in these marlstones and include root traces (Figs. 10C–E).

These variegated and mottled claystones are widespread across the Vistrenque Basin especially in the “Série Rouge” Formation where these form the essential part of this stratigraphic interval but are also frequent in the upper and middle parts of the underlying “Série Mixte” and are also reported in two levels within the “Série Calcaire” Formation (geological reports). In cores, the calcareous claystones are organized into decimetre-to-metre thick intervals the thickness of which may reach up to 2.20 m. These calcareous claystones occur alternating with sandstones (F11), conglomerates (F12) and brecciated limestones (F13 facies, see description hereinafter).

**Interpretation:** The high content of clays and silts in these calcareous claystones indicates settle-out of fine siliciclastic in calm areas (Arenas *et al.*, 2010). The depositional setting may be ephemeral lake and/or floodplain. However, the association of these claystones with the fluvial deposits (F10 and F11) rather suggests floodplain area. The dominant reddish mottling in these calcareous claystones results from the concentration of iron and manganese and indicates reducing conditions during the pedogenesis and later dehydration and oxidation of hydrate minerals which are transformed into crystalline hematite (Tabor *et al.*, 2017).

The presence of root traces within these claystones indicates development of vegetation over the floodplain. Moreover, the alternation of thin sandstone beds with the marlstones suggests overbank deposition. Furthermore, these marlstones are stacked in the form of plurimetre thick intervals; the widespread record of the variegated marlstones across the Vistrenque Basin suggests aggrading floodplain.

### **F13. Nodular-brecciated limestones (pedogenically modified carbonates)**

F13 consists of white-beige brecciated limestones with occasional amounts of siliciclastics and detrital carbonates (Fig. 11A). The lacustrine host rocks may consist of gastropod mudstones to wackestones with ostracod shells and characean remains that display incipient and evolved pedogenic features *sensu* Freydet and Plaziat (1982) resulting in a nodular and brecciated texture. In many cases, the host rock consists of the calcarenites (F7 facies) and intraclastic limestones (F8 and F9 facies) defined previously that display those pedogenic modifications (Figs. 11B–E).

Incipient pedogenesis is expressed by perigranular cracks, weakly differentiated glaebules and sparse root traces. The limestones that are most extensively affected by pedogenesis display abundant and/or enlarged root traces, well developed perigranular cracks but also well differentiated glaebules and pseudomicrokarst features (Fig. 11D). The cavities may reach few centimetres in size and may be filled with bitumen and/or different materials (*e.g.*, ostracodal mudstone).

In thin section, these limestones display dense dark micrite with sparse detrital grains. The perigranular cracks are filled with calcite while the dissolution cavities are filled with geopetal vadose silt and further cemented with blocky calcite spar (Fig. 11C). Beta calcrite fabrics *sensu* Alonso-Zarza and Wright (2010) (*e.g.*, *Microcodium*) are also reported from a few levels (Fig. 11E).

F13 facies occurs mainly in the uppermost part of the “Série Calcaire” Formation and within the *Série Mixte* Formation and is less frequent in the “Série Rouge” Formation. The F13 limestones beds are decimetre-thick and typically cap the plurimetre-thick upward transition from the conglomerates (F10 facies) to quartzose sandstones (F11 facies) and calcareous claystones (F12 facies) in the “Série Mixte” and “Série Rouge” formations. In the “Série Calcaire” Formation, however, pedogenically modified limestones (F13 facies) cap the calcarenite beds (F7 facies) and the intraclastic limestones (F8 and F9 facies).

**Interpretation:** The features observed in F13 facies (perigranular cracks, glaebules, root traces) characterize very shallow lake margin environments subjected to repeated short-term

subaerial exposure (Freydet, 1973; Platt and Wright, 1992). However, pseudomicrokarst features suggest longer duration of subaerial exposure leading to the dissolution of limestones around the root traces resulting in the formation of cavities and further their filling with geopetal silt (vadose silt). Blocky and mosaic cements point to phreatic meteoric environments subsequently to reflooding and burial beneath the overlying sediments.

The occurrence of pedogenically modified carbonates (F13 facies) on top of F7 facies suggests the regression of the lake shoreline and/or progradation of the deltaic system of the lake, and formation of very shallow and ephemeral water bodies. In the same way, pedogenesis modifying the oncolitic and microbial limestones confirms the subaerial exposure of their depositional settings (littoral shoreline). Moreover, the occurrence of F13 palustrine limestones beds in alternation with fluvial conglomerates and sandstones (F10 and F11 facies) and variegated calcareous claystones (F12 facies) is indicative of ephemeral carbonate pond environments developed within the floodplain.

Palustrine limestones are known from semi-arid to subhumid climate settings (Platt and Wright, 1992). Moreover, these authors suggest that microkarst cavities, vadose cements and rhizocretions are characteristic of intermediate climate conditions. Those features, including also *Microcodium*, have been described by Freydet and Plaziat (1982) in the Upper Cretaceous and Lower Tertiary of Languedoc (Southeastern France). Palustrine limestones with nodular-brecciated fabric are also documented in the Priabonian lacustrine deposits from the Issirac Basin (ASCI system, Lettéron *et al.*, 2017).

## **4.2 Facies associations and palaeoenvironmental interpretations**

The vertical distribution of the thirteen depositional facies defined previously in the studied wells allowed to identify six facies associations that enable to infer the depositional environments. The facies associations are: evaporite-rich perennial lake facies association (FA1), profundal lake facies association (FA2), gravity-driven lake slope and offshore lake facies association (FA3), deltaic and littoral lake facies association (FA4), fluvial stream facies association (FA5), palustrine and floodplain facies association (FA6). These facies associations are described hereinafter and summarized in Table 3. The vertical distribution of these facies associations are displayed in Figure 12 for the six studied wells.

**Evaporite-rich perennial lake facies association (FA1)** consists of the anhydritic marls and anhydrite grouped under the facies F1. Based on the petrographic characters, the lack of subaerial exposure evidence, and the alternation with deep lake dark grey marlstones (F3), facies F1 has been shown to form in evaporative perennial saline lake subjected to negative inflow-evaporation balance.

**Profundal lake facies association (FA2)** includes the finely laminated argillaceous limestones and papyraceous marlstones (F2 facies) and the dark grey marlstones with scarce fauna (F3 facies) that indicate deposition in the deep part of a perennial lake with poorly oxygenated waters.

**Lake slope and offshore lake density currents facies association (FA3)** encompasses lacustrine terrigenous-dominated facies (glauconite-rich sandstones and fine calcarenites

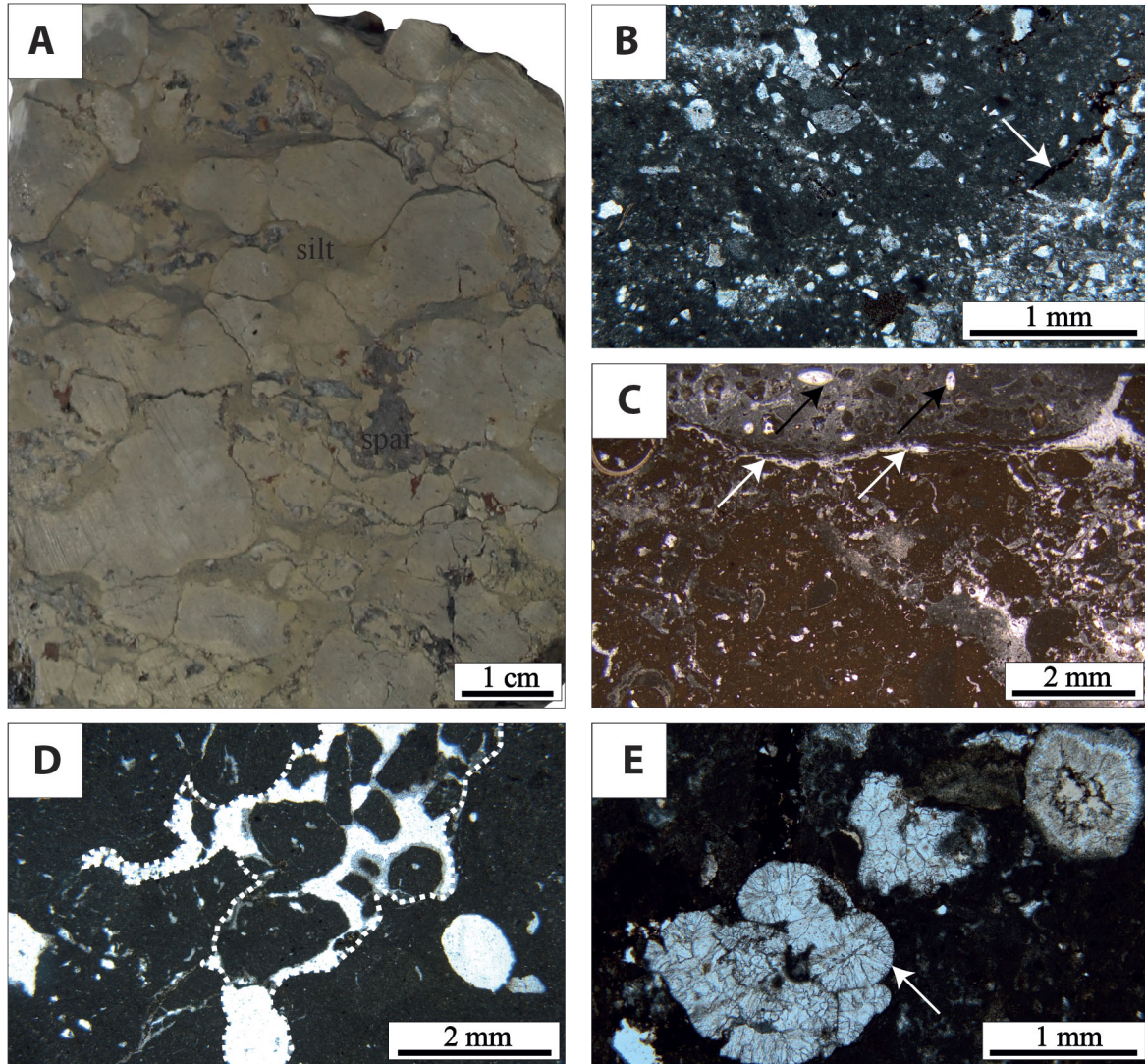


**Fig. 11.** Brecciated and palustrine limestones (F13 facies). (A) Core photograph of a nodular limestone (F13 facies). The nodules (glauabules) are well differentiated indicating long-duration pedogenic processes, the voids between the nodules are filled with silt and blocky calcite (spar). (B) Thin section of a pedogenically modified calcarenite (F7 facies) displaying cracks lined with the clay material (white arrow). This facies is frequent at the top of the F7 calcarenite beds. (C) Thin section of an intraclastic limestone with microbial crusts (F9 facies) displaying subaerial exposure features (silt fill, perigranular cracks (white arrows) around a nodule composed of ostracodal mudstone (black arrows indicate ostracods). (D) Microphotograph showing a conduit (outlined by the dashed line) within a dense dark micrite filled with clasts of the same micrite, resulting probably from the enlargement of a root cavity and filled with glauabules (PPL). (E) Thin section of a palustrine carbonate made of dense dark micrite and showing a well-developed cluster of *Microcodium*.

F4, coarse calcarenites and microconglomerates F5, and conglomerates/breccias F6). The presence of sedimentary structures (*e.g.*, current ripples, parallel laminations, load structures) and the vertical evolution of facies allowed to interpret these facies to be formed in slope and offshore lake conditions (delta front) by gravity-driven currents that evolve downwards from a cohesive flow to a low-density flow. Perennial lake conditions are evidenced from the lack of subaerial exposure features. The terrigenous flux is high during the deposition of these facies and enters the lake in the form of hyperpycnal flow during fluvial floods upstream.

**Deltaic and littoral lake facies association (FA4)** consists of bedded calcarenites (F7), that are sometimes grading into coarse-grained deposits (calcirudites) downwards and fine-grained deposits (calcsiltites) upwards, and of intraclastic limestones (F8-F9). These three facies have been shown to be topped by pedogenically modified limestones (F13 facies). On one hand, the F7 calcarenite beds deposited in the riverine mouth may be affected by pedogenic modifications. The presence of subaerial exposure features and the lack of sedimentary structures related to gravity-driven currents (*e.g.*, parallel laminations, erosive base, load structures) strongly

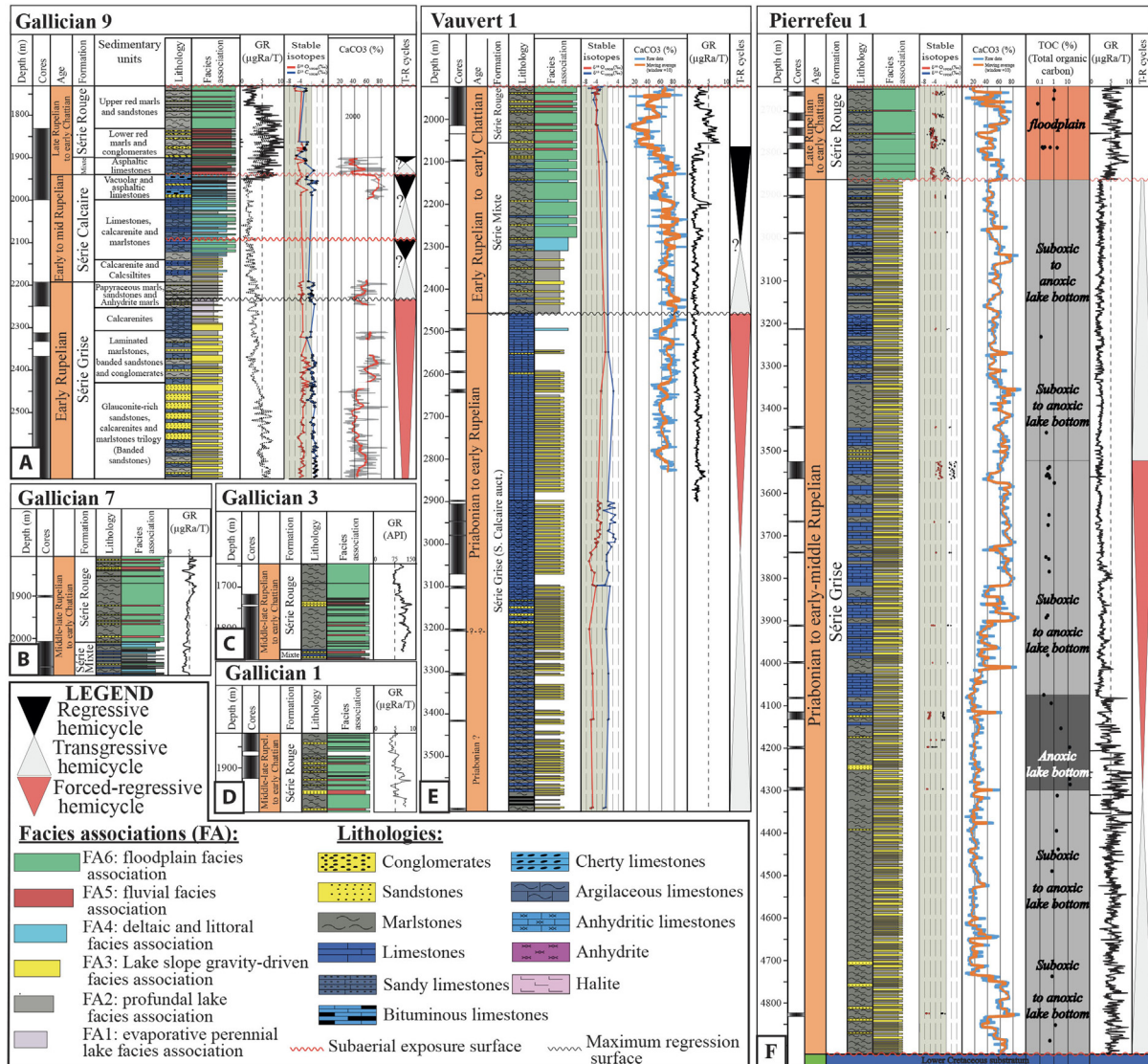


**Fig. 12.** Sedimentary units, lithologies and depositional lithofacies associations and transgressive-regressive cycles of Priabonian (?) to early Chattian deposits from the Vistrenque Basin wells: (A) Gallician 9; (B) Gallician 7; (C) Gallician 3; (D) Gallician 1; (E) Vauvert 1; (F) Pierrefeu 1. See main text for details on facies association definition.

suggest deposition in littoral and deltaic setting, upstream to the FA3 depositional setting. On the other hand, carbonate-rich margin littoral depositional setting is indicated by deposition of oncoliths and reworked intraclasts (tufa fragments) formed in a nearby water spring. FA4 reflects therefore deposition in the vicinity of a riverine mouth where the progradational lake shoreline regression may lead to subaerial exposure of the littoral areas and installation of shallow waterbodies instead (palustrine margin).

**Fluvial facies association** (FA5) comprises the F10 (polymictic conglomerates) and F11 (quartzose sandstones) corresponding to the filling of a channel with both siliciclastic and carbonate clasts. This facies association characterizes fluvial depositional environments probably under high to moderate energy streams (braided to meandering rivers).

**Floodplain facies association** (FA6) consists of variegated and mottled calcareous claystones (F12) and brecciated limestones (F13) with less frequent thinly bedded siliciclastic sandstones (F11). The calcareous claystones may reflect either floodplain deposition or oxidation and decarbonation of lacustrine marls after subaerial exposure. The lack of fauna within these claystones and the occurrence of interbedded overbank sandstones (F11) point to fine particles settlement over the floodplain. The floodplain may be intersected by channels which in turn may be abandoned in the form of ponds and oxbow lakes. The latter ephemeral water pans undergo short-term drying and wetting cycles leading to the development of the F13 palustrine limestones.



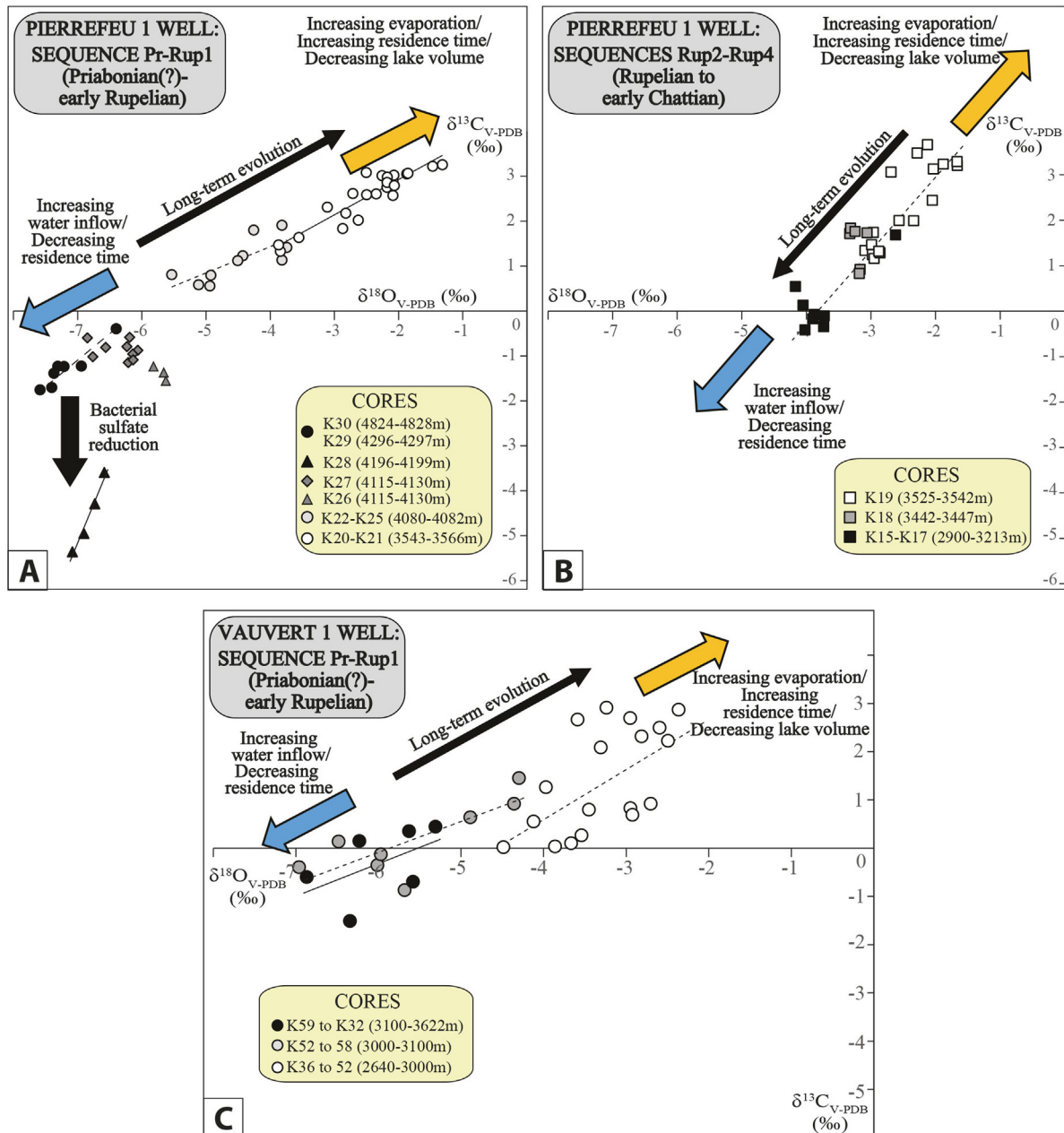


Fig. 13.  $\delta^{13}\text{C}$  and  $\delta^{18}\text{O}$  cross-plots of carbonates from Pierrefeeu 1 well (A, B) and Vauvert 1 well (C) within the “Série Grise” Formation.

### 4.3 Carbon and oxygen stable isotopes signatures of lacustrine carbonates

The dataset used in this chapter is listed extenso in Supplementary data – Table S1. The C&O stable isotopes signatures are graphically illustrated on the multi-well correlation of Figure 12, on the crossplots in Figure 13 and on the panels of Figure 14.

#### 4.3.1 Gallician 9 well

In the “Série Grise” Formation between 2189 m and 2652 m depths,  $\delta^{13}\text{C}$  of bulk rock carbonates values have a

range and vary from  $-1.80\text{‰}$  V-PDB to  $2.05\text{‰}$  V-PDB.  $\delta^{18}\text{O}$  values are also widely distributed since these range between  $-5.02\text{‰}$  PDB and  $-0.54\text{‰}$  PDB (Fig. 13A). Within the “Série Calcaire” Formation, measurements exhibit similar ranges of values of oxygen and carbon stable isotopes ratios as those from the underlying “Série Grise” Unit.  $\delta^{13}\text{C}$  values range from  $-2.03\text{‰}$  PDB while  $\delta^{18}\text{O}$  vary between  $-5.67\text{‰}$  PDB and  $-1.64\text{‰}$  PDB. The bulk-rock geochemical signal from Gallician 9 carbonates is altered by the abundant carbonate detrital fraction and therefore are not considered for palaeohydrological interpretation purposes.

#### 4.3.2 Pierrefeue 1 well

In Pierrefeue 1 well, carbonates from matrix-supported samples (calcareous claystones, marlstones, argillaceous limestone and micritic limestones) from the “Série Grise” formation exhibit a wide range of  $\delta^{13}\text{C}$  (from  $-5.36\%$  to  $+3.83\%$  V-PDB) and  $\delta^{18}\text{O}$  values (from  $-7.59\%$  to  $-1.32\%$  V-PDB) (Fig. 13A). Within the lower interval (4830–4080 m) covered by cores K30 to K26, a positive covariant trend is evidenced at hectometre scale and the lowermost cores (K29 and K30) exhibit moderately negative  $\delta^{13}\text{C}$  values ( $-1.76\%$  to  $-0.39\%$ ) while  $\delta^{18}\text{O}$  values ( $-7.59\%$  to  $-6.40\%$ ) are the most negative within the “Série Grise” Formation. Toward the top of this interval, however,  $\delta^{18}\text{O}$  and  $\delta^{13}\text{C}$  display lesser negative values ( $\delta^{18}\text{O} \sim -6\%$  V-PDB) while  $^{13}\text{C}$  is less important ( $\delta^{13}\text{C} \sim -1\%$  V-PDB). In addition, a positive covariant trend is observed at metre to decametre scale between the  $\delta^{13}\text{C}$  and  $\delta^{18}\text{O}$  signals except for the core K28 made of organic-rich marlstones where  $\delta^{13}\text{C}$  values are very negative ( $-5.36\%$  to  $-3.56\%$  V-PDB) although  $\delta^{18}\text{O}$  values remain similar to the values observed at hectometre scale ( $\sim -7\%$  V-PDB).

From 4000 m (core K25) to 3525 m (core K19) depth, both  $\delta^{13}\text{C}$  and  $\delta^{18}\text{O}$  exhibit an increasing upward trend, the maximum values on top of this interval being respectively  $+3.83\%$  and  $-1.32\%$  (Fig. 13B). Conversely to the underlying interval (4830–4080 m),  $\delta^{13}\text{C}$  values are positive within this interval. Like the 4830–4080 m interval, positive covariant trends are also evidenced between  $\delta^{13}\text{C}$  and  $\delta^{18}\text{O}$  at core (metre to decametre) scale. However, in the upper interval of the “Série Grise” Formation (3447–2900 m: cores K18 to K15), the available dataset suggests an overall slightly decreasing upward trend in both  $\delta^{13}\text{C}$  and  $\delta^{18}\text{O}$ .

#### 4.3.3 Vauvert 1 well

In Vauvert 1 well, carbonates from samples with matrix-supported fabrics exhibit a wide range of  $\delta^{13}\text{C}$  (from  $-3.83\%$  to  $+3.05\%$  V-PDB) and  $\delta^{18}\text{O}$  values (from  $-6.96\%$  to  $-0.79\%$  V-PDB) (Fig. 13C). In the lower part of the studied section (3622–3020 m, cores K62 to K53), available carbon and oxygen stable isotope measurements display apparent low vertical variations with  $\delta^{13}\text{C}$  values ranging from  $-1.51\%$  to  $+0.92\%$  V-PDB and  $\delta^{18}\text{O}$  values from  $-6.87$  to  $-4.36\%$  V-PDB in spite of the relative scarcity of measurements (14 values) within this interval. From 3020 m to 2548 m (cores K52 to K34),  $\delta^{13}\text{C}$  and  $\delta^{18}\text{O}$  values are widely distributed although an overall increasing upward trend in  $\delta^{18}\text{O}$  (up to  $-0.79\%$  V-PDB), a shift toward more positive values (maximum  $\delta^{13}\text{C}$ :  $+3.05\%$  V-PDB) and a roughly positive covariant trend may be observed.

#### 4.3.4 Palaeohydrological interpretation of stable isotope signatures

Covariance of  $\delta^{13}\text{C}$  and  $\delta^{18}\text{O}$  usually occurs in carbonate lake sediments under the condition of long-term hydrological closure, typically for time periods greater than 5,000 yrs (Li and Ku, 1997). Covariant trends have been identified in Pierrefeue-1 at metre-to-decametre scale and likely reflect variations through times of lake hydrological balance and

vapor exchange (Li and Ku, 1997; Leng and Marshall, 2004) in a closed lake. The highest isotopic values reflect high degree of equilibration of the TDIC (Total Dissolved Inorganic Carbon) with atmospheric  $\text{CO}_2$  related to increased water residence time, and preferential evaporative loss of the  $^{16}\text{O}$  (Talbot, 1990; Leng and Marshall, 2004) while the lowest values reflect lower time residence, less evaporated water and therefore isotopic compositions that are closer to those of inflows.

In Vauvert 1 well, a covariant trend is also evidenced but is weak and values are more scattered possibly because of higher and variable concentrations in carbonate detrital particles within the matrix, as also observed in Gallician 9 well, compared to Pierrefeue 1 counterpart: the Vauvert 1 and Gallician 9 wells are located around 3.5 km to the south of Pierrefeue 1 well.

The highly negative  $\delta^{18}\text{O}$  values (down to  $-7.59\%$  V-PDB) evidenced in the lower “Série Grise” Formation in both Pierrefeue 1 and Vauvert 1 wells are consistent with values measured in Priabonian meteoric cements ( $-7\%$  to  $-8\%$  V-PDB) in the Saint-Chaptes Basin (Lettéron *et al.*, 2018). The very negative  $\delta^{18}\text{O}$  values that have been measured in the lower part of the “Série Grise” Formation in Pierrefeue 1 (4830–4080 m) and Vauvert 1 (3622–3020 m) wells suggest relatively short residence time of waters and constant or increasing average lake volume through the considered time interval. In addition, the negative  $\delta^{13}\text{C}$  values in these intervals suggests that the dissolved inorganic carbon from the freshwater inflows was significantly depleted in  $^{13}\text{C}$  which is indicative of a densely vegetated catchment area in a relatively humid climatic setting (Talbot, 1990).

A major break in the vertical evolution of carbon and oxygen isotope compositions of carbonate sediments occurs in Pierrefeue 1 around 4070 m and in Vauvert 1 around 3020 m and which display a significant increase upward and covariant trend of  $\delta^{13}\text{C}$  and  $\delta^{18}\text{O}$ . Within the intervals overlying these depths (*i.e.*, 4000–3525 m in Pierrefeue 1 and 3020–2548 m in Vauvert 1),  $\delta^{13}\text{C}$  values are positive. In these intervals, covariant trends evidenced at metre-to-decametre scale likely reflect high-frequency secular changes of volume of a closed lake while the overall (few hundred metre scale) increasing upward trend in  $\delta^{18}\text{O}$  is indicative of long-term reduction of lake volume.

In Pierrefeue 1 well, the very negative  $\delta^{13}\text{C}$  excursion that occurs in the organic-enriched intervals from the “Série Grise” Formation (K28 core) likely results from  $\text{CO}_2$  released from the organic matter consumption on the lake bottom by sulphate-reducing bacteria as evidenced in other organic-rich lake basins (Carothers and Kharaka, 1980; Kelts and Talbot, 1990). Such sulphate-reduction processes may have been triggered by the development of anoxic conditions on lake bottom as a result of significant organic-matter supply coupled with strengthened water stratification. Water stratification may have been favoured by an increase in lake salinity and associated enhancement of the density difference between the epilimnion and the hypolimnion and thus limiting water mixing and favouring anoxia on lake bottom (*e.g.*, Sonnenfeld, 1985). This interpretation is consistent with the saline nature of the lake during the entire Priabonian and at least episodically during the Rupelian as established by previous studies (Semmani *et al.*, 2022, 2023) and by the coeval onset of

$\delta^{18}\text{O}$  increase which reflects deficient inflow-evaporation balance, lake volume reduction and therefore increased salinity.

Above the organic-rich interval from Pierrefeu 1 well (between 4300 m and 4100 m, TOC (Total Organic Carbon) >5% and up to 10%) and above the depth of 3020 m in Vauvert 1 well, the overall increasing upward trend in  $\delta^{13}\text{C}$  is likely indicative of both higher water residence time and weakly-vegetated catchment area thus strongly suggest dryer climate during the deposition of these intervals. Changes in nature of the substrate of the drainage area through times may also have modified the long-term variation of  $\delta^{13}\text{C}$  of the DIC (Dissolved Inorganic Carbon) and subsequently of the lacustrine carbonates. Finally, the upward decreasing trend in  $\delta^{13}\text{C}$  and  $\delta^{18}\text{O}$  recorded in the upper part of the “Série Grise” from Pierrefeu 1 well (K18-K15: 3447–2900 m) is interpreted to result from a long-term increase in connected volume of lake water.

The analysis of carbon and oxygen isotope compositions of lacustrine carbonates that are common in the “Série Grise” and “Série Calcaire” formations (Priabonian to Middle Rupelian) from both Pierrefeu 1 and Vauvert 1 wells shows that these signals record an overall similar evolution between the two wells. The early stage of lake basin infill (Priabonian to early Rupelian: 4920–4080 m in Pierrefeu 1, 3622–3020 m in Vauvert 1) occurred within a constant or increasing lake volume and is followed by a stage of lake contraction (Early Rupelian: 4080–3525 m in Pierrefeu 1, 3020–2458 m in Vauvert 1). This cycle of long-term lake waxing and waning is followed by a later stage of increasing volume of connected lake water during the early to middle Rupelian times (3525–2860 m in Pierrefeu, 2458–2300 m in Vauvert 1).

#### 4.4 Sedimentary cycles and well correlations

The vertical stacking pattern of facies associations and corresponding depositional environments allow to identify depositional sequences defined as transgressive-regressive (T-R) cycles. The interpretation of T-R cycles has been complemented by the identification of vertical trends of carbon and oxygen isotope ratios of lacustrine micrites from the “Série Grise” and “Série Calcaire” formations. The chronostratigraphic framework used in this section was constructed by Semmani *et al.* (2023) using U/Pb absolute ages and pollen-based climatostratigraphic approaches.

Four medium-scale (few hundreds of metres thick) depositional sequences (Pr-Rup1 to Rup-Ch1) can be defined within the studied units (“Série Rouge” and underlying formations) of the reference section of Gallician 9 well. The depositional sequences described below are shown on the reference section of Gallician 9 and on the sections of the other studied wells (Fig. 12).

##### 4.4.1 Gallician 9 well

###### **Sequence Pr-Rup1: Priabonian (?) to early Rupelian**

In the Gallician sector, the studied wells have not reached the base of the Paleogene. The base of sequence Pr-Rup1 is set at the base of the glauconite-rich interval. The age of the glauconite-rich

interval is not definitely known although pollen data suggest an earliest Rupelian age at the depth of 2530 m. In this sector, the lowermost intervals of the “Série Grise” Formation that are not drilled, hundreds of metres thick according to seismic data (Fig. 2B), may have been deposited as early as the Priabonian (Semmani *et al.*, 2023). The sequence boundary SB1 that separates the Priabonian – Rupelian deposits from the Cretaceous substratum is only known from the Pierrefeu 1 well in the Pierrefeu sector. The glauconite-rich interval is made of a succession of gravity-driven elemental sequences dominated by fine sandstones (low-density turbidites, FA3 association) intercalated with marlstones (FA2) in the lower interval while coarser material (matrix-supported conglomerates, F6 facies) becomes more frequent upwards and dominant in the overlying conglomerates interval. The top of the glauconite-sandstone interval is characterized by chaotically organized conglomerates with lacustrine to palustrine carbonate elements which are likely to be reworked from the lake margins (intraformational clasts), but also by the change of the provenance of the clastic material in the overlying interval. The occurrence of significant amounts of marginal lacustrine clasts reworked within profundal deposits suggests a long-duration subaerial exposition of the lake margins and their subsequent erosion and is therefore consistent with a significant lake regression associated with a major fall in lake level.

Evaporites (FA1 facies association) are abundant in the overlying interval which constitutes the uppermost part of the Pr-Rup1 sequence and indicates the maximum of forced regression of the lake resulting from long-term negative inflow-evaporation balance. The top of the evaporites interval does not display petrographic evidence of subaerial exposure and the FA1 facies association has been shown to form in a perennial evaporative lake. The sequence boundary SB2 which corresponds to the top of the evaporites interval is therefore a maximum regression surface corresponding to the lowermost lake level prior to the water replenishment of the basin at the onset of the deposition of the overlying Rup 2 sequence.

###### **Sequence Rup2: early Rupelian**

Sequence Rup2 overlies the evaporites of the sequence Pr-Rup1. The lower part of the sequence is constituted of alternation of marlstones (FA2) and gravity-driven sandstones (FA3) and corresponds to the upper part of the papyraceous marls interval and the entire calcarenites and calcisiltites interval (2233.4–2140 m): this interval, composed on deep-lake deposits and devoid of evaporites are indicative of a return to a positive inflow-evaporation balance which is consistent with a transgressive hemicycle. FA2 becomes less frequent in the regressive hemicycle which is characterized by upward increase of frequency of the FA4 (F7), and FA6 (F12/F13) facies associations which constitute a thick interval that caps the sequence at the top. The regressive hemicycle therefore records the transition from deep lake conditions (FA2) to deltaic and littoral conditions (FA4) which are accompanied by the development of shallow ephemeral lake and floodplain conditions (FA6). The top of sequence Rup2 is therefore a sequence boundary (SB3) that records the filling of the lake system and subaerial exposure of the lake.

### Sequence Rup3: early to middle Rupelian

Sequence Rup3 is defined between SB3 and the top of the “Série Calcaire” Formation (SB4). In the Gallician 9 well, the lower part is made of alternation of FA4 and FA6 facies associations which represent a return to lacustrine sedimentation, and correspond to the transgressive hemicycle of the lake. This hemicycle is constituted of small-scale sequences of filling of a shallow lake by reworked Mesozoic to Eocene carbonates supplied from the nearby catchment area. Toward the top of this hemicycle, offshore lake conditions are recorded by the frequent marlstones deposits (FA2) that corresponds to the maximum transgression surface. The regressive hemicycle is characterized by an alternation of deep lake (FA2) to deltaic and littoral facies (F7, F8 and F9) that evolves upwards to palustrine deposits at the topmost part. Short-term sequences have been identified within this regressive hemicycle and consist mostly of metre to plurimetre thick lacustrine deltaic and littoral deposits capped by repeated subaerial exposure surfaces. An example of these subaerial exposure surfaces is that dated with U/Pb dating method on calcite which provided an absolute age of  $31.27 \pm 1.90$  Ma for the earliest filling of the microkarst cavities resulting from meteoric diagenesis (Semmani *et al.*, 2023).

The regressive hemicycle of sequence Rup3 is bounded at top by a long-term subaerial exposure surface (SB4) which is marked by drastic changes in sedimentation patterns within the overlying “Série Mixte” and “Série Rouge” formations. The most significant change concerns the nature of the clastic supply origin where crystalline (metamorphic and igneous) sources are involved in the place of local Mesozoic to Eocene carbonate clastic supply.

### Sequence Rup-Ch1: middle-late Rupelian to early (?) Chattian

In the Gallician sector, this sequence corresponds to the “Série Mixte” and “Série Rouge” formations. At the base of the sequence, the “Série Mixte” Formation is bounded by the major subaerial exposure surface SB4 which separates it from the underlying “Série Calcaire” Formation. At top of the sequence, the overlying “Série Rouge” Formation is bounded by a lacustrine flooding surface which separates it from the overlying “Série Calcaréo-Salifère” Formation (Figs. 12A–F).

The base of sequence Rup-Ch1 (“Série Mixte” and “Série Rouge” formations) is characterized by the repetitive occurrence of plurimetre-thick parasequences made of fluvial (FA5) and floodplain (FA6) facies associations, and in less extent profundal lake facies association (FA2). The lower part of the “Série Rouge” Formation is made of alternating fluvial and floodplain deposits (FA5 and FA6) while the upper part records mostly floodplain facies (FA6). The “Série Mixte” Formation records repetitive filling of a shallow lake while the “Série Rouge” indicates rather fluvial and floodplain settings, and the lack of palustrine carbonates is the unique distinguishing feature. In both formations, clastic deposits indicate feeding from the erosion of crystalline rocks. Laterally, the “Série Mixte” Formation was not encountered in the Pierrefeu 1 well and this likely results from lateral variation of facies. However, the thick “Série Rouge” Formation has been encountered in many wells across the Vistrenque Basin and constitutes a correlatable unit. These considerations

suggest that the two units, namely “Série Mixte” and “Série Rouge”, should be grouped in the same depositional sequence.

The lower part of the “Série Mixte” Formation is interpreted to form the transgressive hemicycle of sequence Rup-Ch1, and the maximum transgression can be placed within the lacustrine interval (FA2) close to the formation top. The uppermost part of the “Série Mixte” Formation together with the “Série Rouge” Formation record the regressive hemicycle of sequence Rup-Ch1 with a return to dominant fluvial sedimentation. The fluvial ‘short-term’ sequences recorded in sequence Rup-Ch1 are autocyclic and lateral variations between wells are difficult to capture.

U/Pb dating on calcite at the base of the “Série Rouge” Formation provided an absolute age of  $27.88 \pm 1.71$  Ma (Semmani *et al.*, 2023).

#### 4.4.2 Vauvert 1 well

In a similar way to Gallician 9 well which is located 735 m to the southeast, the “Série Grise” (“Série Calcaire” *auct.*) Formation is dominated in Vauvert 1 well by gravity-driven deep lacustrine carbonate-dominated terrigenous sedimentation. The stable isotope measurements revealed a major break in stable isotope vertical trend around the depth of 3020 m: the increasing  $\delta^{18}\text{O}$  values above 3020 m suggest a long-term negative inflow-evaporation balance and therefore a reduction of lake volume. This event coincides with the occurrence of conglomerate intervals of similar petrographic nature to those observed in Gallician 9 in the lower part of the Pr-Rup1 forced regressive hemicycle. The significant decrease of terrigenous content from 2800 m up to 2458 m (Fig. 14A) is consistent with an important reduction in water inflow and lake volume and therefore point to a correlation of the 2458–3020 m interval from Vauvert 1 well with the Pr-Rup1 forced regressive hemicycle evidenced in the Gallician 9 well.

The interval 2458–2300 m made essentially of gravity driven and profundal lake deposits (FA2 and FA3 facies associations) reflects a transgression of the lake after the forced regression hemicycle. Sedimentation is dominated by deltaic and littoral lake and floodplain deposits (FA4 and FA6 facies associations) within the upper part of “Série Mixte” Formation (2300–2056 m) and by fluvial and floodplain deposits (FA5 and FA6) within the “Série Rouge” Formation (2056–1922 m). This upward transition toward the installation of a floodplain is indicative of an overall normal lake regression as evidenced in the Rup 2 to Rup 3 sequences previously described in Gallician 9 well. The scarcity of core data in the “Série Mixte” Formation (2056–2458 m) in Vauvert 1 well prevents from the identification of the boundaries of sequences Rup 2, Rup 3 within this package: these sequences are here merged into one single lower-order transgressive-regressive sequence (Figs. 12E and 14A).

#### 4.4.3 Pierrefeu 1 well

As in Gallician 9 and Vauvert 1 wells, the lower part of the “Série Grise” shows frequent gravity-driven deep lacustrine terrigenous deposits. Stable isotope signatures allowed to identify a major turnover in lake paleohydrology between 4300 and 4070 m depths and the onset of long-term negative inflow-evaporation balance conditions which are persistent up to

around 3525 m. The significant reduction in terrigenous supplies within the 4300 m–3525 m interval as evidenced by core observations and by a decrease in gamma-ray (Fig. 14B) and an increase in CaCO<sub>3</sub> content is consistent with a decrease in terrigenous sediment inputs associated with a decrease in water inflow and therefore with a long-term negative inflow-evaporation balance. This interval may therefore be considered to correlate with the forced regressive hemicycle of sequence Pr-Rup 1 described in the Gallician-9 section. The lower interval (4920–4300 m) therefore corresponds to the transgressive hemicycle of sequence Pr-Rup 1.

Above this level, the interval 3525–2860 m (upper part of the “Série Grise”) is constituted of a monotonous succession of alternating gravity-driven deposits and profundal marls (FA2 and FA3 facies associations). Such a vertical succession together with the nearly constant to slightly decreasing trend in  $\delta^{13}\text{C}$  and  $\delta^{18}\text{O}$  signals suggest a long-term increase of connected volume of lake water, consistent with a transgressive trend (Fig. 14B). The sharp lithological change supported by Gamma Ray signal shift at the contact between the top of the “Série Grise” and the overlying “Série Rouge” Formation and the lack of lateral equivalent of the “Série Calcaire” and “Série Mixte” formations described in Gallician 9 well (Fig. 4) strongly suggest the occurrence of a normal fault intersecting the well. Nevertheless, the long-term evolution of the sedimentation in the Pierrefeu sector is similar to that in the Gallician sector and the upward transition to the floodplain deposits of the “Série Rouge” Formation suggest an overall normal regression of the lake. As in Vauvert 1, sequences Rup2 to Rup3 have been merged into a single transgressive-regressive cycle (Figs. 12F and 14B).

## 5 Discussion

### 5.1 Depositional models for the Paleogene lacustrine succession

The analysis of the vertical stacking pattern of the studied sedimentary succession (“Série Rouge” and underlying units) and the lateral relationships of the defined depositional facies associations within the correlatable sedimentary units enable to construct three depositional models that characterize the infill of the Vistrenque Basin from the Priabonian to late Rupelian-early Chattian times (Fig. 15): (1) profundal freshwater to oligohaline lake, (2) perennial evaporative lake, and (3) shallow lake with extensive floodplain, depending on tectonic, climatic, and hydrological setting.

#### Profundal freshwater to oligohaline lake: Figure 15A

FA2 and FA3 facies associations indicate profundal lake setting subjected to high clastic supply. Their dominance in transgressive/stillstand hemicycle and lowermost part of regressive hemicycle of sequence Pr-Rup1 and transgressive hemicycle of sequence Rup2 allows to reconstruct for these intervals a profundal lake depositional model and assess the clastic and water supplies, water salinity, topography, bedrock composition and tectonic setting.

The abundance of FA3 in these sequences indicates high clastic fluxes entering the lake system. Clastic fluxes are transported into the lake system by fluvial streams and

therefore a significant riverine freshwater input enters the lake during the deposition of these gravity-driven deposits in the profundal areas. The deposition of cohesive debrites and turbidites in the lake slope and bottom accompanies hyperpycnal flows and the water inflow therefore resulted in lake transgression. Riverine inputs that feed the lake mostly drain igneous and metamorphic rocks from the southern Pyrenean reliefs and Mesozoic marine carbonates from the neighbouring of the lake. Such meteoric-derived river streams most likely consist of freshwater. However, oligo-mesohaline conditions in the northern margin of the Priabonian lake at Butte Iouton evidenced by Semmani *et al.* (2022) strongly suggest contribution by saline water, albeit very diluted by riverine freshwater inputs, in the central and southern parts of the lake, particularly in Pierrefeu and Gallician sectors.

The high clastic fluxes entering the lake indicate important weathering upstream in the catchment area. In the lower units (“Série Grise” Formation) from the Gallician area, the nature of the clasts (*e.g.*, marine carbonates, glauconite mineral) suggests detrital feeding from the erosion of the Mesozoic cover that forms the bedrock of the catchment area. The monomictic nature of the matrix-supported conglomerates suggests dominant clastic supply from the surroundings and indicates that far crystalline basement constitutes a less dominant source for the feeding of clastic material. The “Série Grise” Formation overlies unconformably the Mesozoic cover constituted at top by the Albian glauconite sandstones, and the Neocomian (Lower Cretaceous) and Jurassic marine carbonates which provide the detrital material to the lake. Compared to the Gallician counterpart, sedimentation is dominated by fine grained deposits in the Pierrefeu sector which may constitute the distal area of the basin.

Moreover, the abundance of plant debris (leaves, stems) within the FA3 facies association suggests dense vegetation cover in the surroundings of the lake. Dense vegetation cover and high riverine inflows are consistent with relatively humid conditions. The lack of subaerial exposure features (*e.g.*, perigranular cracks, root traces, dissolution cavities) within these units strongly suggests persistence of perennial lake conditions. In addition, the persistently very negative  $\delta^{18}\text{O}$  values of carbonate matrix in the “Série Grise” Formation (Fig. 14), close to those of calcite precipitated from meteoric waters within the neighbouring Priabonian Saint-Chaptes Basin (Lettéron *et al.*, 2018) support also significant freshwater supplies (riverine, groundwater and/or precipitation). The covariant trends between  $\delta^{18}\text{O}$  and  $\delta^{13}\text{C}$  are consistent with increased water residence times (Fig. 13).

On the other hand, FA2 facies association, especially the laminated argillaceous limestones and papyraceous marlstones (F2 facies) suggest lake stratification and deposition in deep poorly oxygenated lake bottom (Platt and Wright, 1991). Water stratification may result from thermal or density processes. Stratification may be enhanced by the saline nature of the water and by seasonal evaporation of the surface waters (epilimnion). Deposition of marlstones and argillaceous limestones during low clastic supply periods suggests a tendency for hydrological lake closure. Organic matter preservation in the lake bottom is consistent with the water stratification, poor oxygenation of lake bottom, and perennial lake conditions.

The thicknesses of the transgressive and stillstand hemicycle (223 m) and lower part of regressive hemicycle

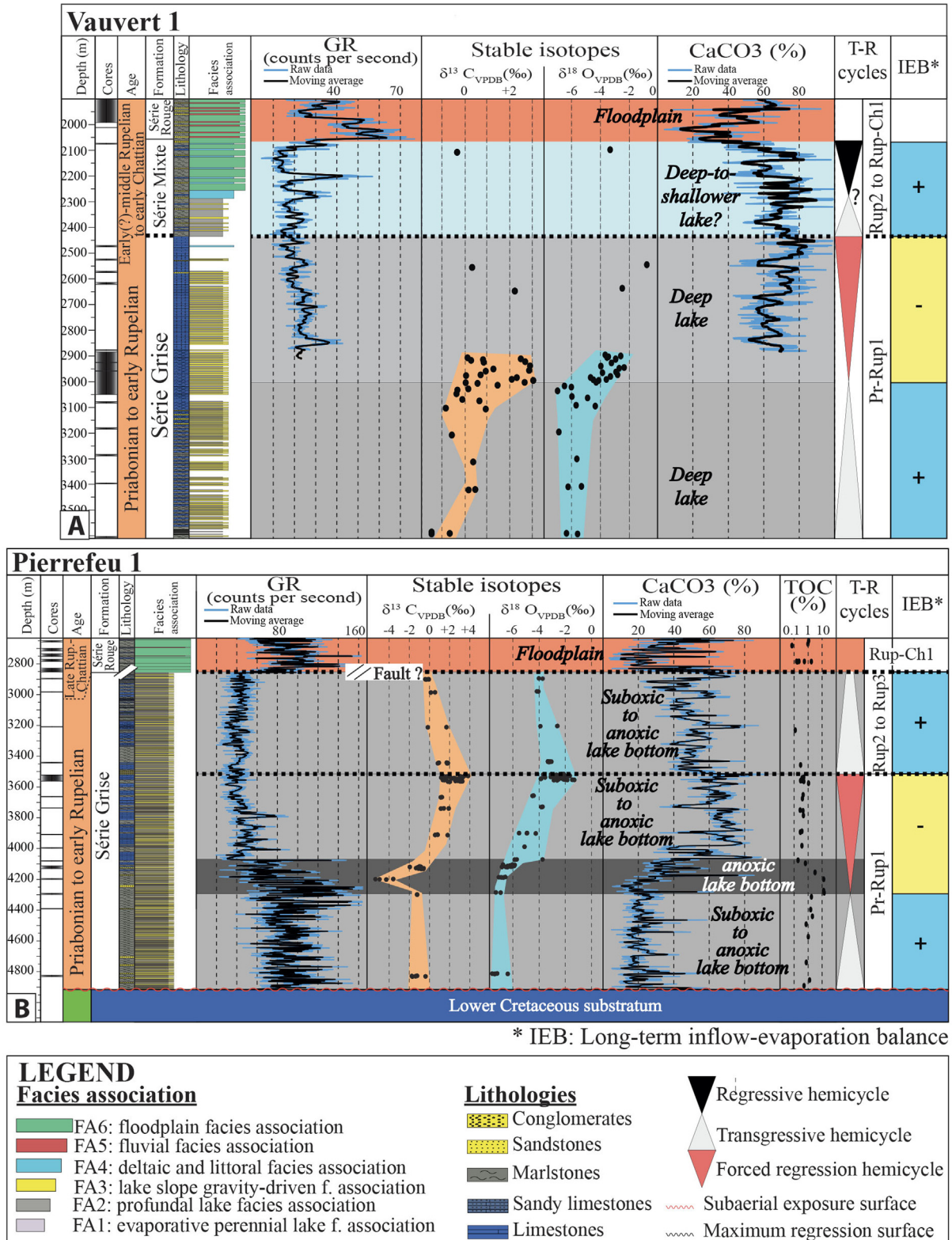


**Fig. 14.** Synthetic panel of vertical variations in  $\delta^{18}O$ ,  $\delta^{13}C$ ,  $CaCO_3$  content, Gamma Ray signal, TOC (Total Organic Carbon), and the interpreted lacustrine transgressive and regressive trends and long-term inflow-evaporation balance: A: Vauvert 1 well; B: Pierrefeuf 1 well.

(145 m) of sequence Pr-Rup1 and of the transgressive hemicycle (93 m) of sequence Rup2 in the reference section of Gallician 9 well are important and these thicknesses are found to be much more important in the Pierrefeü 1 well. These intervals are characterized by monotonous accumulation of interbedded gravity driven deposits with profundal lake marls without any evidence of subaerial exposure. This stacking pattern reflects persistence of deep lake conditions in the studied areas (Gallician and Pierrefeü sectors). The persistence of deep lake conditions and steep lacustrine slope allowing deposition of hectometre scale turbidite stacks may result from the absence of a topographic sill in the lake system that would result in water outflow and/or from a high subsidence rate leading to continuous creation of accommodation space and keeping the studied area in profundal lake conditions during these time intervals.

Finally, these intervals from Sequences Pr-Rup 1 (transgressive/stillstand and lower regressive hemicycle) and Rup 2 (transgressive hemicycle) were formed within a freshwater to oligohaline highly subsiding lake system comprising a slope break into the bottom and fed by high siliciclastic and carbonate detrital inputs from the southern Pyrenean reliefs and from the neighbouring highs of the catchment area within humid to semi-humid conditions (Fig. 15A).

#### Perennial evaporative lake: Figure 15A

In Gallician 9 well, FA1 facies association is the dominant facies association within the upper part of the regressive hemicycle of Sequence Pr-Rup1 with FA2 and FA3 found in lesser extent. The alternation of anhydrite with organic-rich grey marlstones in the evaporative interval and the lack of subaerial exposure evidence allowed to interpret their formation within perennial evaporative lake conditions. Hypersaline conditions and arid climate are required to precipitate these evaporites (gypsum and anhydrite). Concentration of solutes into brine results in water stratification. Stratified waters are associated with poorly oxygenated bottom, and this is consistent with the preservation of organic matter in the anhydritic marls (F1 facies).

The lack of evaporites in the correlative levels from Vauvert 1 and Pierrefeü 1 suggests transient disconnection between lake waters from Gallician 9 area and those from deeper areas in the lake basin. This is consistent with a tectonic compartmentalization of the basin controlling the lake bottom topography and with the formation of a localized evaporative ponded areas developing on the hanging-wall of a tilted block. For instance, the compartmentalization between the Gallician and Pierrefeü sectors may likely be caused by the Gallician transfer zone that separates the Marsillargues and Vauvert compartments (Fig. 2A). The forced regression of the lake and the significant reduction of the clastic fluxes into the lake bottom strongly suggest a very negative inflow-evaporation balance. No direct information is available about the expression of the forced regression surface in the lake margins, but the occurrence of reworked ooids, of similar size, shape, and structures with those from the Priabonian northern lake margin (Butte Iouton, Semmani *et al.*, 2022) in the upper regressive hemicycle of sequence Pr-Rup1 reflects exposure

and incision of the Priabonian to Rupelian lake margins during the early Rupelian forced regression.

The deposition system in which the regressive hemicycle of sequence Pr-Rup1 formed is therefore a perennial, saline to hypersaline, profundal lake subjected to dryer climate conditions and to reduced clastic gravity-driven flux and the depositional area of evaporites is plausibly disconnected from the main waterbody by an emerged crest of tilted block (Fig. 16).

#### Shallow lake with extensive floodplain: Figure 15B

In the regressive hemicycles of sequence Rup2, and the entire sequences Rup3 and Rup-Ch1, facies associations FA4, FA5 and FA6 are dominant and indicate lacustrine littoral delta, fluvial and floodplain settings (Fig. 15B). Profundal lake deposits such as organic-rich marls are rare and correspond to the maximal expansion of the lake. In contrast to the perennial profundal lake system described previously, this lacustrine system is rapidly and repeatedly filled and exposed. These rapid fluctuations of the shoreline are evidenced by the frequent subaerial exposure surfaces and pedogenesis occurring at top of plurimetre-thick shallow lake sequences. The almost lack of gravity driven deposits (FA3) and dominance of marginal lacustrine facies (FA4) suggest a gentler basin topography. Moreover, the lack of laminated marlstones and the poor preservation of organic matter suggests a non-stratified water body which is consistent with the shallow water conditions.

Pedogenic carbonates occur in semi-arid to semi-humid conditions. The presence of pseudomicrokarst features in the “Série Calcaire” and “Série Mixte” formations is indicative of intermediate climate conditions (Platt and Wright, 1992). The abundance of lacustrine detrital calcarenites in the top of “Série Calcaire” Formation and the upward transition to floodplain deposits suggests progradation of an alluvial system into the lake. Alluvial and deltaic progradation and infill of the lake system may have been promoted by slowing of subsidence.

In sequences Rup3 and Rup-Ch1, the dominant siliciclastic fluxes strongly suggest uplift and erosion of crystalline rocks. The crystalline basement that constitutes the continuation of the French-Spanish Pyrenees to the east covers large areas to the south of the Vistrenque Basin, in place of the present Gulf of Lion and therefore may have acted as a source of igneous and metamorphic clasts into the lake. The increasingly important involvement of far crystalline sources compared to the nearby Mesozoic marine carbonates suggests low relief creation in the margins of the lake and therefore slowdown of the erosion of these rocks. Low topography creation, *i.e.*, slow subsidence across the Vistrenque Basin allowed the progradation of far detrital fluxes into the lacustrine system.

In conclusion, the sedimentary system of the marginal lacustrine and fluvial to floodplain deposits of the regressive hemicycle of sequence Rup2 and sequences Rup3 and Rup-Ch1 consists of a shallow lake subjected to both carbonate and siliciclastic terrigenous fluxes under semi-arid to semi-humid conditions and undergoing frequent subaerial exposure (Fig. 15B). An analogue of a such mixed fluvio-lacustrine systems is known in the basal Cretaceous from the Central northern Spain Rupelo formation of the Western Cameros Basin (Platt, 1989 in Platt and Wright, 1992) where abundant

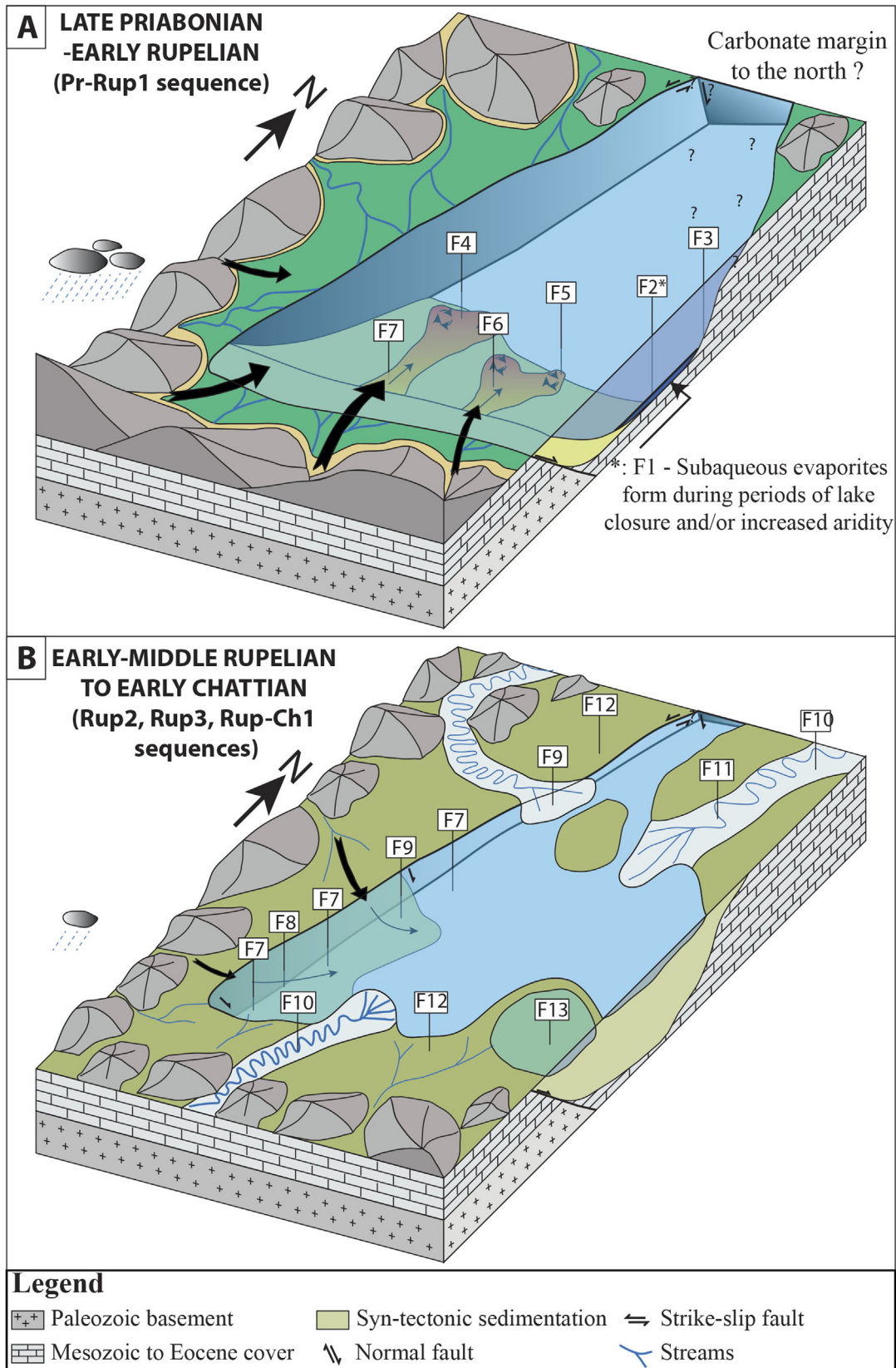


**Fig. 15.** Simplified block diagrams showing the depositional models for (A) profunderal perennial lake, and (B) shallow lake with extensive floodplain. Evaporites (F1 facies) formed within perennial lake conditions precipitate in compartmentalized areas with maximum reduction of connection to the main saline waterbody (see Fig. 16 for further details).



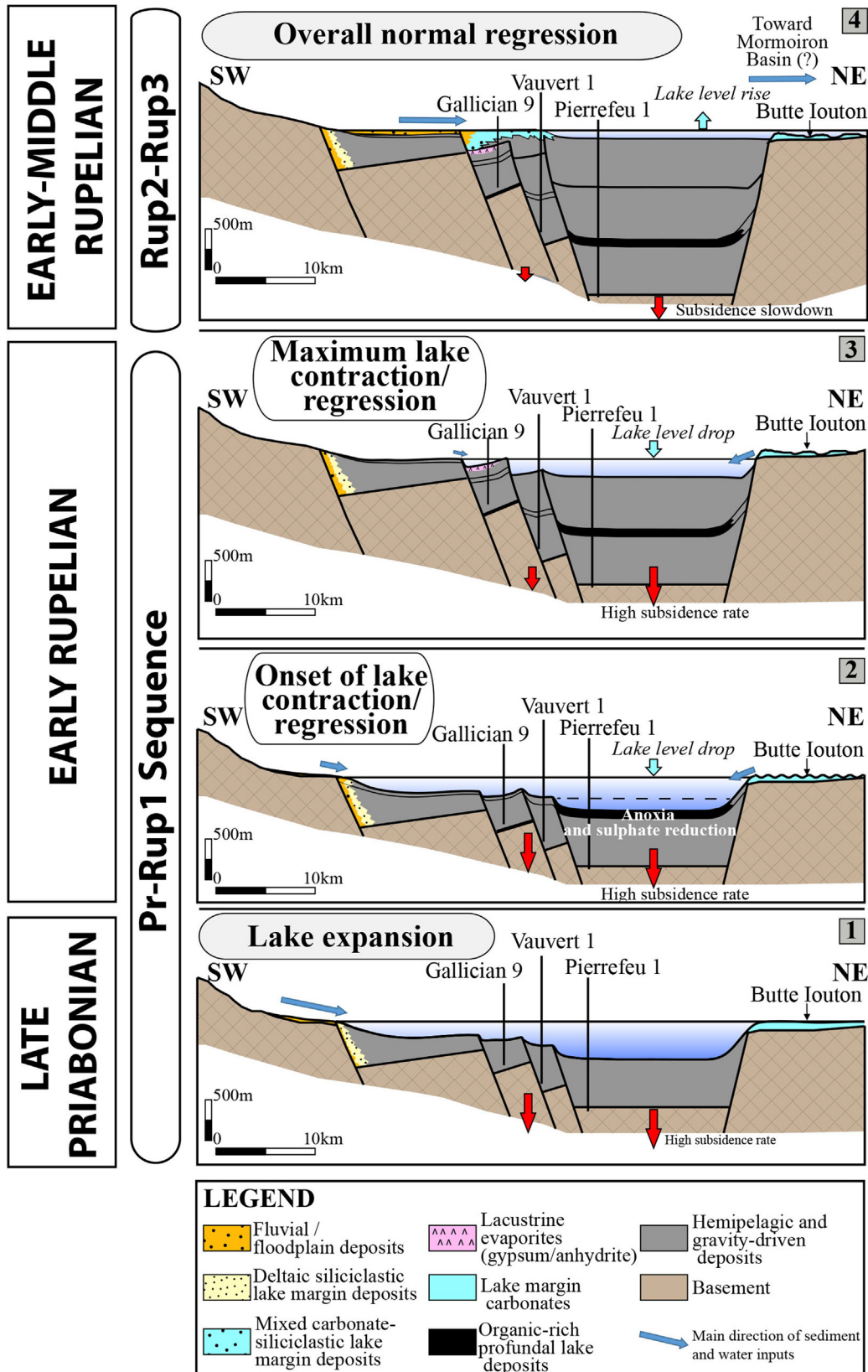


**Fig. 16.** Conceptual model of the sedimentary infill of the Vistrenque lacustrine system from the Priabonian (?) to early Chattian as a function of palaeohydrological and tectonic setting. Sequences Pr-Rup1, Rup2, Rup3 and Rup-Ch1 are defined from the Gallician 9 well reference section.

marlstones (calcareous claystones) of red and green colours are abundant in the alluvial setting and floodplain near a low energy gentle slope margin.

## 5.2 Tectonic and climatic controls on the Paleogene Vistrenque Basin infill during the late Priabonian and early-mid Rupelian

In the Vistrenque Basin, the present study shows a significant development of clastic gravity-driven sedimentation, especially in the southern part of the basin (Gallician sector). In the Pierrefeu sector, these deposits are more fine-grained, and this polarity trend suggests a dominant SSW-to-NNE direction of sedimentary fluxes. Detrital fluxes sourced from the south are documented in the neighbouring Sommières, Saint-Chaptes and Alès basins during the Priabonian (Rémy, 1985; Rémy and Fournier, 2003; Lettéron *et al.*, 2018, 2022).

In contrast to these Languedoc siliciclastic fluxes, the almost monogenic character of the carbonate extraclasts in the lower part of the Vistrenque Paleogene infill suggests significant involvement of the Mesozoic cover from the surroundings of the basin in the supply of sedimentary fluxes to the depositional system. The nature of the sedimentary fluxes is consistent with the nature of the basin substratum revealed in the wells. The substratum is Early Cretaceous in age to the North and the West, while the Lower Cretaceous cover is absent to the South and to the East in the Grau-du-Roi-Saintes-Maries-de-la-Mer and Albaron highs (Figs. 2A, 2C).

The thick accumulation of gravity-driven deposits (hectometre scale units) during the Priabonian (?) and early Rupelian required both a strong subsidence to create the space for sedimentation and significant water inflows into the basin. The Vistrenque Basin is controlled by the Nîmes Fault that acted as a sinistral strike-slip fault within the NNE-SSW trending Languedoc fault belt during the Priabonian (Séranne *et al.*, 2021). Furthermore, only an important basin structuration resulting from high subsidence rates and the absence of an outlet sill of the system allows to maintain profundal lake conditions where sedimentation does not take pace with the accommodation. Very steeply subsiding topographies commonly characterize pull-apart basins (*e.g.*, Platt and Wright, 1992, Smit *et al.*, 2008) and this is consistent with the strike-slip motion of the Nîmes Fault during Priabonian and early Rupelian times as mentioned above although normal fault motions would have occurred in relation to the Western European Rift extension. This basin configuration allows to account for the hectometre-scale monotonous succession of alternating FA2/FA3 facies associations in the slope and deepest areas of the lake system (Fig. 16). Periods of important extensive tectonic activity have favoured creation of a strong topography following the uplift of the footwall in the surroundings and consequently their erosion favoured by enhanced precipitation that promote the development of coarse-grained gravity-driven fluxes (FA3). Conversely, periods of low water inflows lead to a decrease in terrigenous inputs and therefore favour carbonate production in the lake (FA2 facies association). FA2 and FA3 are formed in the deeper parts of the lake, the lateral evolution of facies is

difficult to quantify in terms of changes in the depth of the depositional area.

A striking aspect of the Vistrenque Basin lake evolution is the development of deep gravity facies since the earliest stage of the sedimentation, as suggested by the turbidites of the base of the “Série Grise” in Pierrefeu 1, overlying the Mesozoic substratum. This suggests that a deep topographic depression was already existing prior to its infill by water and prior lacustrine sedimentation. During the Priabonian to earliest Rupelian transgression/stillstand, some marginal areas of the Vistrenque Basin (at least around Butte Iouton to the North and Puech du Teil to the West: Semmani *et al.*, 2022) were occupied by a shallow water lake margin with carbonate sedimentation showing high-frequency cycles of transgression and forced regression which suggest the occurrence of short episodes of negative inflow-evaporation balance in a period of mainly sub-humid climate. Finally, the high terrigenous fluxes, the persistence of a perennial deep-lake setting as well as the stable isotope signatures of deep-lake carbonates strongly suggest a relatively humid climate setting during the late Priabonian in the Vistrenque Basin (Fig. 17). This is consistent with palaeoclimatic reconstructions from sedimentologic and palaeobotanic data of the late Priabonian in the Alès and Saint-Chaptes basins (Tanrattana *et al.*, 2020; Lettéron *et al.*, 2022; Semmani *et al.*, 2023).

The onset of the forced regressive hemicycle identified from the depositional and stable isotope records in Gallician 9, Vauvert 1 and Pierrefeu 1 wells is situated around 100 m above a pollen flora characterizing the Priabonian-Rupelian climatic deterioration in Vauvert 1 (3200 m depth: location 5 in Fig. 17), and around 100 m above another pollen flora, earliest Rupelian in age, in Gallician 9 (2530 m depth: location 6 in Fig. 17). The latter reflects a stage of significant precipitation decrease during the earliest Rupelian times (Semmani *et al.*, 2023). The present dataset suggests therefore that the Eocene-Oligocene transition (EOT) and the earliest Rupelian ‘aridification’ evidenced from pollen records held just prior to the effective reduction in lake volume and lacustrine forced regression. In Pierrefeu 1 well, located in the most subsiding profundal area of the lake, the stage of lacustrine forced regression starts with the deposition of organic-rich horizons (TOC > 10%) associated with <sup>13</sup>C depleted isotope composition which suggests sulphate-reduction processes (Fig. 12F, 13A, 14B). Sulphate reduction processes are linked to enhanced water stratification likely resulting from increased salinity (*e.g.*, Sonnenfeld, 1985). Vauvert 1 and Gallician 9 did not record such organic-matter enrichment and sulphate-reduction processes because of their shallower depositional settings and of prevailing more oxygenated waters. In Pierrefeu 1 well, the decrease in organic matter concentrations in lake bottom sediments in the later stages of forced regression is likely to be related to the decrease in terrestrial organic matter into the lake consequent to the continental slight aridification and the reduction of vegetation cover in the catchment area. Compared with the late Priabonian pollen floras from the Alès Basin (Maruéjols 1 well 798 m location 3 in Fig. 17, Montchamp location 4 in Fig. 17), pollen data from Vauvert 1 (3200 m) and Gallician 9 (2530 m) indicate that the vegetation change was characterized by a strong decrease in tropical plants and strengthening of open environments including Ephedra as shrub marker of less humid conditions (Ickert-Bond and Renner, 2016).

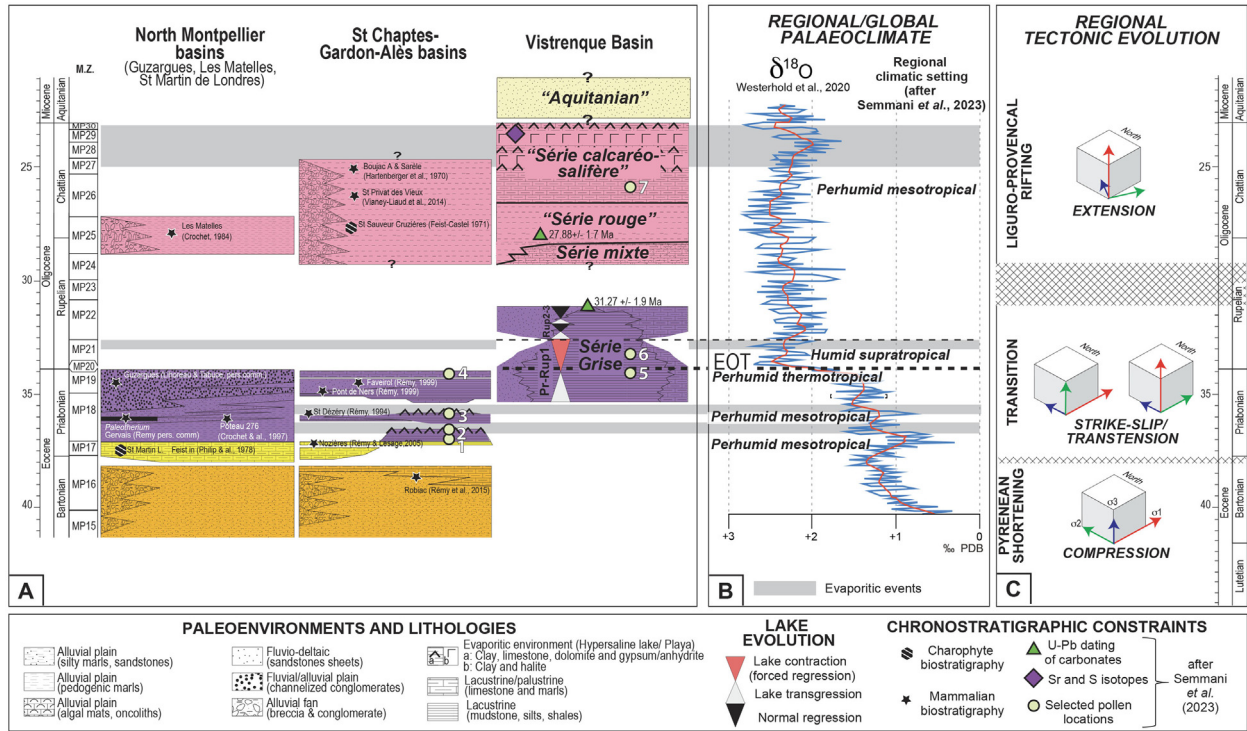


**Fig. 17.** (A) Correlation chart of the Bartonian to Aquitanian deposits from the North-Montpellier, Alès-Saint-Chaptes and Vistrenque basins, and inferred ages. Biostratigraphy scale is based on mammal reference levels (M.Z.). Ages from North-Montpellier and Alès-Saint-Chaptes basins are based on fossil mammal and charophytes biostratigraphy. The chronostratigraphic framework from the Vistrenque basin is based on U-Pb datings on carbonate minerals, Sr and S isotopes and pollen-based climatostratigraphy (Semmani *et al.*, 2023). Dominant palaeoenvironments and lithologies of the formations are indicated. White areas correspond to non-depositional and erosional hiatuses. The Priabonian interval from Alès-Saint-Chaptes basins is documented in Lettéron *et al.* (2018, Lettéron 2022) and North-Montpellier basin stratigraphy is based on Séranne *et al.* (2021). (B) Benthic foraminiferal oxygen isotope curve (smoothed curve over 20ka in blue, smoothed curve over 1Ma in red; after Westerhold *et al.*, 2020) reflecting the global climate evolution and Priabonian to Chattian regional palaeoclimate characterization (according to Fauquette *et al.*, 1998a) recorded in southern France basins (Semmani *et al.*, 2023). (C) Evolution of the regional tectonic setting from the late Eocene to earliest Miocene in southern France. The hatched area represents an uncertainty in the time interval separating successive tectonic stages. Pollen sample locations (after Semmani *et al.*, 2023): 1: Euzet Hill, 2: Serre de Cauvel 3; 3: Maruéjols-1 798m; 4: Montchamp; 5: Vauvert-1 well 3200m; 6: Gallician-9 well 2530m; 7: Gallician-1 well 1648m.

The occurrence of evaporites in Gallician 9 well and their absence in the more profundal settings of the Vauvert 1 and Pierrefeu 1 areas suggest transient disconnection of the depositional area of Gallician 9 from the main water body during the maximum of lake regression (Fig. 16). The combination of available pollen data, the depositional features identified in the studied wells and the chronostratigraphic constraints strongly suggest that a significant reduction of lake volume occurred during the early Rupelian and is associated with a stage of significant decrease in precipitation. Even though most studies regarding palaeoclimatic changes in European terrestrial environments during the EOT have shown a significant decrease in mean annual temperature around the Priabonian-Rupelian boundary (Mosbrugger *et al.*, 2005; Erdei *et al.*, 2012; Hren *et al.*, 2013; Tanrattana *et al.*, 2020), evidence for critical change in precipitation at a large geographic scale remains unclear. However, a southward gradient of drier conditions has been suggested for the Oligocene period from a synthesis of palaeobotanical studies despite their high heterogeneity (Utescher *et al.*, 2021). Indeed,

most of information come from macrofloras from which quantified reconstructed palaeoclimatic parameters are somewhat less robust compared with those obtained from pollen data (Girard *et al.*, 2019). In addition, only few pollen data considered in this synthesis are valid for palaeoclimatic reconstructions for their weak approach in botanical identification and/or incomplete pollen counting. On the contrary, our dataset represents a robust, multiproxy evidence of some 'aridification' in terrestrial environment in Southeast France during the early Rupelian following the EOT transition. The link between global cooling and regional lowering in precipitation is not straightforward and requires detailed palaeo-relief and wind reconstructions to be established. However, the available palaeogeographic reconstructions for southeast France during the Paleogene (Joseph and Lomas, 2004; Semmani *et al.*, 2023) suggest that decrease in lake volume during the early Rupelian results from decreased precipitation associated with global oceanic cooling and decreased regional moisture around the western Alpine Sea. The classification of present-day bioclimates with respect both

to mean annual temperature (MAT) and mean annual precipitation (MAP) established by Fauquette *et al.* (1998a) (Supplementary materials: Table S3) allows to characterize the environmental evolution of Southeast France through seven selected pollen locations encompassing the EOT according to climate reconstructions proposed by Semmani *et al.* (2023) (Fig. 17; Supplementary materials: Table S4).

Gravity sedimentation in lakes downstream of an important hydrographic network carries significant water fluxes during the humid periods. The transgression of the lake system and its connection with neighbouring saline water bodies followed by less humid period explains the formation of the lacustrine basin evaporites. Compared to other continental basins in the Western European Rift system (*e.g.*, Valence Basin, Bresse Basin, Upper Rhine Graben and in less extent the Manosque Basin; Rouchy, 1997) where evaporites records are significant during the Rupelian, evaporites are scarce in the southern part of the rift system constituted by the Camargue area and are limited to the early Rupelian Stage of global cooling and associated continental aridification.

The overlying sequence Rup2 marks the end of evaporitic conditions in Gallician 9 well and a return to a terrigenous-rich, gravity-driven sedimentation and to a long-term positive inflow-evaporation balance. Such an inversion in palaeohydrological balance is interpreted to be related to a potential a return to wetter conditions on the continent following the brief stage of cooling that occurred during the earliest Rupelian times (Westerhold *et al.*, 2020) (Fig. 17).

The occurrence of deep-water gravity-driven sediments become less frequent toward the top of Rup2 sequence in Gallician 9 and shallow, marginal lacustrine sedimentation dominates in sequence Rup3 while sequence Rup-Ch1 is characterized by the development of floodplain environments in the studied wells from the Vistrenque Basin that intersect the “Série Rouge” and “Série Mixte” formations (Gallician 1, 3, 7, 9, Vauvert 1, and Pierrefeu 1 wells). Since the palaeohydrological balance remains positive during the middle to late Rupelian interval, such a palaeoenvironmental vertical evolution may suggest either an increase in terrigenous supplies or a decrease in subsidence rates. The latter interpretation is more likely since the vertical disappearance of gravity-driven sediments could be related to gentle basin topography following a slowing down of subsidence and fault activity. In addition, an increase in terrigenous supplies is unlikely since the southern Pyrenean reliefs which are believed to have sourced a large proportion of the sediment were probably less elevated during the mid-late Rupelian compared to the late Priabonian to early late Rupelian. This elevation decrease is consistent with the collapse of this Pyrenean segment that started as early as the Priabonian south to the Languedoc area (Séranne *et al.*, 2021). Moreover, reconstruction of terrestrial precipitation (Semmani *et al.*, 2023; Supplementary materials: Table S4) suggest that the mid-late Rupelian climate was not as humid as during the Priabonian.

Finally, the overall shallowing upward trend recorded in sequences Rup2 to Rup3 combined with the upward decreasing trend in  $\delta^{18}\text{O}$  and  $\delta^{13}\text{C}$  which is indicative of long-term positive inflow-evaporation balance and therefore of an increase in connected lake volume, suggests that the Vistrenque Basin was likely connected to a neighbouring waterbody, and that the terminal fluvial plain system probably

flowed into another lake located further north (Mormoiron and/or Apt-Manosque-Forcalquier basins).

### 5.3 A record of the transition from Pyrenean shortening to Liguro-Provençal rifting?

The age of the onset of the Liguro-Provençal rifting is regionally assumed to be late Rupelian or early Chattian (Séranne, 1999). In the neighbouring North Montpellier basins, mammalian fossil assemblages (Crochet, 1984; Séranne *et al.*, 2021) allow constraining the onset of the rifting phase during or prior to the MP25 horizon (27.3–28.8 Ma after Gradstein, 2012). The Priabonian to early-middle Rupelian age of the “Série Grise” and “Série Calcaire” in the Vistrenque Basin, as inferred from U-Pb datings and pollen-based climatostratigraphy (Semmani *et al.*, 2023), strongly suggests a pre-rift deposition (Fig. 17). Moreover, the extremely thick Pr-Rup1 lacustrine sequence (up to 1400 m) accumulated within less than 3.5 Myrs is indicative of a deposition in a highly subsiding basin. Strike-slip movement of the Nîmes Fault, bordering the Vistrenque Basin, has been evidenced from the Priabonian sedimentation in the neighbouring North-Montpellier and Saint-Chaptes-Alès basins (Séranne *et al.*, 2021). The partly coeval, thick lacustrine sequences (Pr-Rup1, Rup2 and Rup3) forming the “Série Grise” and “Série Calcaire” in the Vistrenque Basin are therefore likely to have deposited in a transtensional basin resulting from the strike-slip movement of the Nîmes Fault during a transitional stage between the Pyrenean shortening and the Liguro-Provençal rifting (Fig. 17).

In contrast, the available age for the “Série Rouge” ( $27.88 \pm 1.7$  Ma) may be consistent with a syn-rift deposition. Additionally, the karstification of the limestone at the top of Rup3 and the available U-Pb age below SB4 ( $31.27 \pm 1.9$  Ma; Semmani *et al.*, 2023) may support a potential significant time gap below the overlying “Série Mixte”.

A major change in the nature of terrigenous inputs above SB4 surface suggests a significant shift in drainage areas and/or river orientation in response to the onset of the Liguro-Provençal rifting. The occurrence of metamorphic and igneous elements in the “Série Mixte” and “Série Rouge” formations may be indeed related to sediment supplies from the Massif Central located northwest of the Vistrenque Basin and to southward sediment transport directions. However, this change may also be related to a complete abrasion of the Mesozoic sedimentary cover on the southern Pyrenean reliefs and subsequent erosion of the crystalline basement.

The preservation of a relatively thick alluvial plain succession (“Série Rouge”) suggests a phase of significant accommodation creation, more in line with a subsiding basin rather than passive infill. The “Série Rouge” Formation is almost isopacheous across the basin (Fig. 12) with a thickness averaging 200 m, which is consistent with a deposition in a symmetric graben in contrast with the younger Aquitanian fan-shaped, syn-rift sequence evidenced from seismic profiles by Benedicto *et al.* (1996) and associated with the development of a half-graben controlled by the Nîmes Fault.

In the overlying “Calcaréo-salifère” Formation (Fig. 4), Chattian in age, strontium and sulphur isotope signatures of evaporites revealed seawater influx which is likely related to

marine connections with the Western Neotethys to the south during the Liguro-Provençal rifting phase (Semmani *et al.*, 2023). Finally, the thick, fan-shaped, clastic sediment wedge overlying the “Calcaréo-salifère” Formation (Fig. 2B), assigned to the Aquitanian were interpreted as representing the main stage of rift basin development in the Vistrenque area (Benedicto *et al.*, 1996; Séranne, 1999).

Finally, the available sedimentologic, stratigraphic and geochronologic results suggest that the “Série Mixte” and “Série Rouge” formations (Rup-Ch1 sequence: late-Rupelian to Chattian) likely deposited either during a phase of tectonic quiescence subsequent to the strike-slip motion of the Nîmes Fault and/or during an early stage of the Liguro-Provençal rifting (Fig. 17).

## 6 Conclusion

Sedimentological and stratigraphic analysis of the Paleogene succession from the Vistrenque Basin (Camargue area) integrating carbon and oxygen isotope measurements on lacustrine carbonates and total organic carbon (TOC) data allowed to document a case of the record of changes in climate and tectonic setting around the Eocene-Oligocene transition in a continental basin from Southwestern Europe.

- Three depositional sequences (Pr-Rup1 to Rup3) have been defined within the Priabonian to early-mid Rupelian of the Vistrenque Basin. To account for the several hectometres thick stack of turbidites in the depocentre of the Vistrenque Basin, the sedimentary system consisted of a highly subsiding profundal freshwater to oligohaline lake which was fed with significant clastic fluxes and riverine inflows during the transgressive hemicycles of sequences Pr-Rup1 and Rup2 where the lake waterbody has recorded its maximum expansion.
- Local deposition of evaporites within the Vistrenque Basin during the early Rupelian provides further evidence for the continental record of the brief phase of decreased precipitations inferred from previous pollen analyses. These evaporites occur at the top of the forced regressive stage of sequence Pr-Rup1 which is defined by the vertical evolution of facies and confirmed by a long-term increase in both  $\delta^{18}\text{O}$  and  $\delta^{13}\text{C}$  signatures of lacustrine carbonate matrices. Such a forced regression trend has been identified and correlated between three wells located in distinct tectonic blocks and is interpreted to result from a decrease in lake volume in response to decreased precipitation associated with global oceanic cooling and decreased regional moisture around the western Alpine Sea. This brief early Rupelian continental ‘aridification’ stage is followed by a return to more humid conditions during the deposition of the transgressive hemicycle of sequence Rup2 from the early-middle Rupelian as indicated by an increase in terrigenous inputs resulting into the desalinization of the lake and long-term decrease of both  $\delta^{18}\text{O}$  and  $\delta^{13}\text{C}$  signatures.
- The regressive hemicycle of sequence Rup2 and the following sequences Rup3 and Rup-Ch1 record an upward transition from deep-lacustrine lake settings to a gently steeping shallow lake characterized by important marginal lacustrine and palustrine environments and by an upward

increase of floodplain and fluvial deposits reflecting an overall regressive trend of the lake system between the early-middle Rupelian and early Chattian times.

- The thick succession (up to 2000 m) of Priabonian to early-middle Rupelian deep-lacustrine gravity-driven deposits reflects sedimentation in a highly subsiding basin during a stage of strike-slip and transtension motions of the Nîmes Fault. The marginal lacustrine and floodplain deposits within the upper part of the Paleogene Vistrenque Basin infill (“Série Mixte” and “Série Rouge”: Rup-Ch1 sequence) accumulated during a phase of tectonic quiescence subsequent to the strike-slip motion of the Nîmes Fault and/or during an incipient stage of the Liguro-Provençal rifting.

## Supplementary material

**Table S1:** Carbon and oxygen isotopes ratios of the samples from Gallician 9, Vauvert 1 and Pierrefeu 1 wells, KB: Kelly bushing (zero reference for driller’s depth measurements).

**Table S2:** Total organic carbon (TOC) measurements from Pierrefeu 1 well.

**Table S3:** Classification of bioclimate according to mean annual temperature (MAT) and mean annual precipitation (MAP) (Fauquette *et al.*, 1998).

**Table S4:** Reconstructed climate parameters and bioclimate characterization from some selected pollen records (Semmani *et al.*, 2023).

In bold characters, the most likely value (MLV, for more details, see Fauquette *et al.*, 1998b).

The Supplementary Material is available at <https://www.bsgf.fr/10.1051/bsgf/2024005/olm>.

## Acknowledgments

This work was funded by the France’s Ministry of Higher Education and Research and is part of the PhD of the first author. This work also benefited from the financial supports of CEREGE (APIC 2018 RRH), Carb3E TotalEnergies-AMIDEX Chair and INSU (project EOT-Climate funded by the TelluS-Syster Program) and we thank them profoundly for their support. We would like to thank TotalEnergies for providing in-house documents as a part of the data sharing agreement (Contract of cooperation and data exchange TotalEnergies – Aix-Marseille University FR00040451). The authors would also thank Gilles Graffin (STC core library, Boussens) who gave access to cores from the Camargue wells. The authors are grateful to Christophe Nussbaumer (TotalEnergies) for his review of the manuscript and for his suggestions and comments.

## References

- Alonso-Zarza AM, Wright VP. 2010. Chapter 5 Calcretes. *Developments in Sedimentology* The Netherlands: Elsevier 61: 225–267.
- Arenas C, Cabrera L, Ramos E. 2007. Sedimentology of tufa facies and continental microbialites from the Paleogene of Mallorca Island (Spain). *Sediment Geol* 197: 1–27.

- Arenas C, Vazquez-Urbez M, Pardo-Tirapu G, Sancho-Marcen C. 2010. Chapter 3 Fluvial and associated Carbonate deposits. *Developments in Sedimentology* 61: 133–175.
- Arthaud F, Laurent P. 1995. Contraintes, déformation et déplacement dans l'avant-pays Nord-pyrénéen du Languedoc méditerranéen. *Geodyn Acta* 8: 142–157.
- Ashley GM, Renaut RW. 2002. Rift sedimentation. In Renaut RW, Ashley GM, eds. *Sedimentation in Continental Rifts, SEPM Special Publication* Tulsa, USA. 73 pp. 3–10.
- Basilici G. 1997. Sedimentary facies in an extensional and deep-lacustrine depositional system: the Pliocene Tiberino Basin, Central Italy. *Sediment Geol* 109: 73–94.
- Blanc-Valleron M-M., Schuler M. 1997. Paleogene evaporitic basins of Alsace (Southern Rhine Graben). In Busson G, Schreiber B, eds. *Sedimentary deposition in rift and foreland basins in France and Spain*. New York: Columbia University Press, pp. 85–135.
- Benedicto A. 1996. Modèles tectono-sédimentaires de bassins en extension et style structural de la marge passive du golfe du Lion (Partie Nord), Sud-est France. Université de Montpellier II. Thèse de doctorat, 249pp.
- Benedicto A, Labaume P, Séguret M, Séranne M. 1996. Low-angle crustal ramp and basin geometry in the Gulf of Lion passive margin: the Oligocene-Aquitainian Vistrenque graben, SE France. *Tectonics* 15: 1192–1212.
- Bestani L, Espurt N, Lamarche J, Floquet M, Philip J, Bellier O, Hollender F. 2015. Structural style and evolution of the Pyrenean-Provence thrust belt, SE France. *Bull Soc Géol France* 186: 223–241.
- Bouma AH. 1962. *Sedimentology of some Flysch deposits; A graphic approach to facies interpretation* Elsevier, Amsterdam 168 pp.
- Carothers WW, Kharaka YK. 1980. Stable carbon isotopes of  $\text{HCO}_3^-$  in oil-field waters—implications for the origin of  $\text{CO}_2$ . *Geochem Cosmochim Acta* 44: 323–332.
- Crochet J-Y. 1984. Géologie et paléontologie de la partie septentrionale du fossé oligocène des Matelles (Hérault, sud de la France). *Géol France* 1-2: 91–104.
- Crochet JY, Hartenberger J., Rémy JA, Sudre J, Welcome JL. 1997. Découverte de vertébrés continentaux de l'Eocène moyen et supérieur dans le bassin des Matelles (Hérault, Sud de la France) et redécouverte du « Lophiodon des Matelles ». *Géol France* 1: 35–45.
- Curial A, Moretto R. 1997. The Salt Basin of Bresse: Southern Saône Graben. In Busson G, Schreiber BC eds. *Sedimentary Deposition in Rift and Foreland Basins in France and Spain*. New York: Columbia University Press, pp. 136–194.
- Dromart G, Dumas D. 1997. The salt basin of Valence (France). In Busson G, Schreiber BC, eds. *Sedimentary Deposition in Rift and Foreland Basins in France and Spain*. New York: Columbia University Press, pp. 195–239.
- Dunham RJ. 1962. Classification of carbonate rocks according to depositional texture. In: Ham WE, ed., *Classification of Carbonate Rocks*. Tulsa: AAPG pp. 108–121.
- Eldrett JS, Greenwood DR, Harding IC, Huber M. 2009. Increased seasonality through the Eocene to Oligocene transition in northern high latitudes. *Nature* 459: 969–973.
- Embry AF, Klovan JE. 1971. A late devonian reef tract on Northeastern Banks Island. *Can Petrol Geol* 19: 730–781.
- Erdei B, Utescher T, Hably L, Tamas J, Roth-Nebelsick A, Grein M. 2012. Early oligocene continental climate of the palaeogene basin (Hungary and Slovenia) and the surrounding area. *Turk J Earth Sci*: 21: 2(Article 1).
- Espitalié J, Deroo G, Marquis F. 1985. La pyrolyse Rock-Eval et ses applications – Première partie. *Rev l'Inst Franç Pétrole* 40: 563–579.
- Fabre J, Mainguet M. 1991. Continental sedimentation and palaeoclimates in Africa during the Gondwanian Era (Cambrian to Lower Cretaceous): the importance of wind action. *J Afr Earth Sci* 12: 107–115.
- Fauquette S, Quézel P, Guiot J, Suc JP. 1998a. Signification bioclimatique de taxons-guides du Pliocène méditerranéen. *Geobios* 31: 151–169.
- Fauquette S, Guiot J, Suc JP. 1998b. A method for climatic reconstruction of the Mediterranean Pliocene using pollen data. *Palaeogeogr Palaeoclimatol Palaeoecol* 144: 183–201.
- Freytet P. 1973. Petrography and paleoenvironments of continental carbonates deposits with a particular reference to Upper Cretaceous and Lower Eocene of Languedoc, Southern France. *Sediment Geol* 10: 25–60.
- Freytet P, Plaziat JC. 1982. Continental carbonate sedimentation and pedogenesis – Late Cretaceous and Early Tertiary of Southern France. In: Purser BH Ed., *Contribution to Sedimentology, Schweizerbartsche Verlag, Stuttgart*, 12, 217 pp.
- Girard V, Fauquette S, Adroit B, Suc JP, Leroy SAG, Ahmed A, Paya A, Ali AA, Paradis L, Roiron P. 2019. Fossil mega- and micro-flora from Bernasso (Early Pleistocene, southern France): a multimethod comparative approach for paleoclimatic reconstruction. *Rev Palaeobot Palynol* 267: 54–61.
- Gorini C, Le Marrec A, Mauffret A. 1993. Contribution to the structural and sedimentary history of the Gulf of Lions (western Mediterranean), from the ECORS profiles, industrial seismic profiles and well data. *Bull Soc Géol France* 164: 353–363.
- Hartenberger JL, Sigé B, Sudre J, Vianey-Liaud M. 1970. Nouveaux gisements de Vertébrés dans le Bassin tertiaire d'Alès (Gard). *Bull Soc Géol France* 7: 879–885.
- Hren MT, Sheldon ND, Grimes ST, Collinson ME, Hooker JJ, Bugler M, Lohmann KC. 2013. Terrestrial cooling in Northern Europe during the Eocene-Oligocene transition. *Proc Natl Acad Sci USA* 110: 7562–7567.
- Joseph P, Lomas S. 2004. Deep-water sedimentation in the Alpine Foreland Basin of SE France: new perspectives on the grès d'Annot and related systems – an introduction. In Joseph P, Lomas S, eds. *Deep-water sedimentation in the Alpine Foreland Basin of SE France: new perspectives on the grès d'Annot and related systems, The Geological Society of London, Special Publications* 1, pp 1–16.
- Kelts K, Talbot M. 1990. Lacustrine carbonates as geochemical archives of environmental change and biotic/abiotic interactions. In Tilzer M, Colette S, eds. *Large Lakes: Ecological Structure and Function*. Springer pp. 288–315.
- Lehn I, Fallgatter C, Kern H.P, Sergio Gomes S Paim P. 2018. Co-genetic, cohesive and non-cohesive delta front facies: a case study of flow transformation in a lacustrine setting, Camaquã Basin, southernmost Brazil. *J South Am Earth Sci* 86: 271–286.
- Leng MJ, Marshall JD. 2004. Palaeoclimate interpretation of stable isotope data from lake sediment archives. *Quat Sci Rev* 23: 811–831.
- Lesueur JL. 1991. Etude sédimentologique et stratigraphique du Bassin Paléogène d'Apt-Manosque-Forcalquier (Alpes de Haute Provence). Modalités de la transition Burdigalienne. Ph.D. thesis, University M. de Montaigne, Bordeaux III, France, 407 pp.
- Lettéron A, Fournier F, Hamon Y, Villier L, Margerel J-P, Bouche A, Feist M, Joseph P. 2017. Multi-proxy paleoenvironmental reconstruction of saline lake carbonates: Paleoclimatic and

- paleogeographic implications (Priabonian-Rupelian, Issirac Basin, SE France). *Sediment Geol* 358: 97–120.
- Lettéron A, Hamon Y, Fournier F, Séranne M, Pellenard P, Joseph P. 2018. Reconstruction of a saline, lacustrine carbonate system (Priabonian, St-Chaptes Basin, SE France): depositional models, paleogeographic and paleoclimatic implications. *Sediment Geol* 367: 20–47.
- Lettéron A, Hamoun Y, Fournier F, Demory F, Séranne M, Joseph P. 2022. Stratigraphic architecture of a saline lake system: From lake depocenter (Alès Basin) to margins (Saint-Chaptes and Issirac basins), Eocene-Oligocene transition, south-east France. *Sedimentology* 69: 651–695.
- Li HC, Ku L. 1997.  $\delta^{13}\text{C}$  –  $\delta^{18}\text{O}$  covariance as a paleohydrological indicator for closed-basin lakes. *Palaeogeogr Palaeoclimatol Palaeoecol* 133: 69–80.
- Lowe DR. 1982. Sediment gravity flows: II. Depositional models with special reference to the deposits of high-density turbidity currents. *J Sedimentol Soc Econ Paleontol Mineralog* 52: 279–297.
- Lowe DR, Guy M. 2000. Slurry-flow deposits in the Britannia Formation (Lower Cretaceous), North Sea: a new perspective on the turbidity current and debris flow problem. *Sedimentology* 47: 31–70.
- Masclé A, Jacquart G, Deville E. 1994. The Corbières transverse zone of the Pyrenee-Provence thrust belt (south France) – Tectonic history and petroleum plays. 6th Conference, *European Association of Petroleum Geoscientists & Engineers*, Extended Abstract, P556, Vienna, 1994.
- Mosbrugger V, Utescher T, Dilcher DL. 2005. Cenozoic continental climatic evolution of Central Europe. *Proc Natl Acad Sci* 102: 14964–14969.
- Orti F, Salvany JM. 2004. Coastal saline evaporites of the Triassic-Liassic boundary in the Iberian Peninsula: The Alacón borehole. *Geol Acta* 2: 291–304.
- Page M, Licht A, Dupont-Nivet G, Meijer N, Barbolini N, Hoorn C, *et al.* 2019. Synchronous cooling and decline in monsoonal rainfall in northeastern Tibet during the fall into the Oligocene icehouse. *Geology* 47: 203–206.
- Peckmann J, Paula J, Thiel V. 1999. Bacterially mediated formation of diagenetic aragonite and native sulfur in Zechstein carbonates (Upper Permian, Central Germany). *Sediment Geol* 126: 205–222.
- Pellat E, Allard M. 1895. Dépôts lacustres de la Butte Iouton entre Comps et Beaucaire (Gard). *Bull Soc Géol France* 23: 434–436.
- Pentecost A. 2005. Travertine. Springer Berlin, Heidelberg, New York 446 pp.
- Platt NH. 1989. Lacustrine carbonates and pedogenesis: sedimentology and origin of palustrine deposits from the Early Cretaceous Rupelo Formation, W Cameros Basin, N Spain. *Sedimentology* 36: 665–684.
- Platt NH, Wright VP. 1991. Lacustrine carbonates: facies models, facies distribution and hydrocarbon aspects. *Spec. Publs Int Ass Sediment* 13: 57–74.
- Platt N.H, Wright VP. 1992. Palustrine carbonates and the Florida Everglades; towards an exposure index for the fresh-water environment? *J Sediment Petrol* 62: 1058–1071.
- Rémy JA. 1985. Nouveaux gisements de mammifères et reptiles dans les grès de Célas (Éocène sup. du Gard). Etude des paléothériidés (Perissodactyla, Mammalia). *Palaeontogr Abteilung A* 189: 171–225.
- Rémy JA. 1994. Une faunule de vertébrés sous la base des Grès de Célas (Eocène sup.) à Saint-Dézéry (Gard). *Palaeovertebrata* 23: 211–216.
- Rémy JA. 1999. Deux nouveaux gisements de Vertébrés fossiles dans la formation de Célas (Éocène supérieur du Gard). *Bulletin de la Société des Sciences Naturelles de Nîmes et du Gard* 62: 16–22.
- Remy JA. 2015. Les Périssodactyles (Mammalia) du gisement Bartonien supérieur de Robiac (Éocène moyen du Gard, Sud de la France). *Palaeovertebrata* 23: 211–216.
- Rémy JA., Fournier F. 2003 Un nouveau gisement de vertèbres d'âge Priabonien et son contexte géologique (Tranchée de Nozieres, Gard). *Bulletin de la Société des Sciences Naturelles de Nîmes et du Gard* 64: 18–30.
- Rémy JA, Lesage JL. 2005. Mammifères fossiles de Grès de Célas (Éocène supérieur du Gard) : Découvertes récentes. *Bulletin de la Société des Sciences Naturelles de Nîmes et du Gard* 65: 7–15.
- Rouchy JM. 1997. Paleogene continental rift system of Western Europe: locations of basins, paleogeographic and structural framework, and the distribution of evaporites. In: Busson G Schreiber BC Eds. *Sedimentary Deposition in Rift and Foreland Basins in France and Spain*. New York: Columbia University Press, pp. 45–94.
- Semmani N, Fournier F, Léonide P, Feist M, Boularand S, Borgomano J. 2022. Transgressive-regressive cycles in saline lake margin oolites: paleogeographic implications (Priabonian, Vistrenque Basin, SE France). *BSGF Earth Sci Bull* 193: 8.
- Semmani N, Fournier F, Suc J-P., Fauquette S, Godeau N, Guihou A, Popescu SM, Melinte-Dobrinescu MC, Thomazo C, Marié L, Deschamps P, Borgomano J. 2023. The Paleogene continental basins from SE France: new geographic and climatic insights from an integrated approach, *Palaeogeogr Palaeoclimatol Palaeoecol* 615: 111452.
- Séranne M. 1999. The Gulf of Lion continental margin (NW Mediterranean) revisited by IBS: an overview. In: Durand B, Jolivet L, Horváth F, Séranne M Eds. *The Mediterranean basins: Tertiary extension within the Alpine Orogen*. Volume Special Publication 156 London: The Geological Society, pp. 15–36.
- Séranne M, Benedicto A, Truffert C, Pascal G, Labaume P. 1995. Structural style and evolution of the Gulf of Lion Oligo-Miocene rifting: role of the Pyrenean orogeny. *Mar Petrol Geol* 12: 809–820.
- Séranne M, Couëffé R, Husson E, Baral C, Villard J. 2021. The transition from Pyrenean shortening to Gulf of Lion rifting in Languedoc (South France) – A tectonic-sedimentation analysis. *BSGF – Earth Sci Bull* 192: 27.
- Smit J, Brun JP, Cloetingh S, Ben Avraham Z. 2008. Pull-apart basin formation and development in narrow transform zones with application to the Dead Sea Basin. *Tectonics* 27: TC6018.
- Sonnenfeld P. 1985. Evaporites as oil and gas source rocks. *J Petrol Geol* 8: 253–271.
- Tabor NJ, Myers TS, Michel LA. 2017. Sedimentologist's guide for recognition, description, and classification of Paleosols. *Terrestre Depos Syst* 165–208.
- Talbot MR. 1990. A review of the palaeohydrological interpretation of carbon and oxygen 1121 isotopic ratios in primary lacustrine carbonates. *Chem Geol* 80: 261–279.
- Talling PJ, Masson DG, Sumner EJ, Malgesini G. 2012. Subaqueous sediment density flows: depositional processes and deposit types. *Sedimentology* 59: 1937–2003.
- Tanner L. 2010. Continental Carbonates as Indicators of Paleoclimate. *Dev Sedimentol* 62: 179–214.
- Tanrattana M, Boura A, Jacques F, Villier L, Fournier F, Enguehard A, Cardonnet S., Volland G, Garcia A, Chaouch S, De Franceschi D. 2020. Climatic evolution in Western Europe during the Cenozoic:

- insights from historical collections using leaf physiognomy. *Geodiversitas* 42: 151–174.
- Tinterri R, Magalhaes PM, Tagliaferri A, Cunha RS. 2016. Convolute laminations and load structures in turbidites as indicators of flow reflections and decelerations against bounding slopes. examples from the Marnoso-arenacea Formation (northern Italy) and Annot Sandstones (south eastern France). *Sediment Geol* 344: 382–407.
- Tinterri R, Civa A, Laporta M, Piazza A. 2020. Chapter 17 – Turbidites and turbidity currents. In: Scarselli N, Adam J, Chiarella D, Roberts DG, Bally AW Eds. *Regional Geology and Tectonics* (Second Edition). Elsevier, pp. 441–479.
- Utescher T, Erdei B, François L, Henrot, AJ, Mosbrugger V, Popova S. 2021. Oligocene vegetation of Europe and western Asia-Diversity change and continental patterns reflected by plant functional types. *Geolog J* 56: 628–649.
- Valette M. 1991. Etude structurale du gisement salifère Oligocène de Vauvert (Gard), *Thèse de doctorat*, Univ. Montpellier II, 229 pp.
- Valette M, Benedicto A. 1995. Chevauchements gravitaires halotectoniques dans le bassin distensif de Camargue (marge du golfe du Lion, SE de la France). *Bull Soc Géol France* 166: 137–147.
- Vianey-Liaud M, Comte B, Marandat B, Peigné S, Rage JC, Sudre J. 2014. A new early Late Oligocene (MP 26) continental vertebrate fauna from Saint-Privat-des-Vieux (Alès Basin, Gard, Southern France). *Geodiversitas* 36: 565–622.
- Viles HA, Taylor MP, Nicoll K, Neumann S. 2007. Facies evidence of hydrodynamic regime shifts in tufa depositional sequences from the arid Naukluft Mountains, Namibia. *Sediment Geol* 195: 39–53.
- Wentworth CK. 1922. A scale for grade and class terms for clastic sediments. *J Geol* 30: 377–392.
- Westerhold T, Marwan N, Drury AJ, Liebrand D, Agnini C, Anagnostou E, Barnet JSK, Bohaty SM, De Vleeschouwer D, Florin D, Lauretano V, Littler K, Lourens LJ, Lyle M, Pälike H, Röhl U, Tian J, Wilkens RH, Wilson P.A, Zachos JC. 2020. An astronomically dated record of Earth's climate and its predictability over the last 66 million years. *Science* 369: 1383–1387.
- Ziegler PA. 1992. European Cenozoic rift system. In: Ziegler PA Ed. *Geodynamics of Rifting, Volume I, Case History Studies on Rifts: Europe and Asia. Tectonophysics* 208: 91–111.

**Cite this article as:** Semmani N, Fournier F, Suc J-P, Fauquette S, Séranne M, Léonide P, Marié L, Borgomano J. 2024. Continental depositional record of climate and tectonic evolution around the Eocene-Oligocene transition in southeast France: perspectives from the Vistrenque Basin (Camargue), *BSGF - Earth Sciences Bulletin* 195: 8.